

000 001 002 003 004 005 006 007 008 009 010 011 012 013 014 015 016 017 018 019 020 021 022 023 024 025 026 027 028 029 030 031 032 033 034 035 036 037 038 039 040 041 042 043 044 045 046 047 048 049 050 051 052 053 MIXTURE OF COGNITIVE REASONERS: MODULAR REASONING WITH BRAIN-LIKE SPECIALIZATION

006 **Anonymous authors**

007 Paper under double-blind review

010 ABSTRACT

013 Human cognitive behavior arises from the interaction of specialized brain net-
014 works dedicated to distinct functions, such as language, logic, and social reason-
015 ing. Inspired by this organization, we propose Mixture of Cognitive Reasoners
016 (MiCRO): a modular, transformer-based architecture post-trained with a curricu-
017 lum that induces functional specialization across experts. Concretely, we partition
018 the layers of a pretrained language model into four expert modules aligned with
019 well-studied cognitive networks in the human brain. MiCRO offers three key
020 advantages over standard language models. (1) The specialized experts are in-
021 terpretable and causally meaningful—ablating a module causes substantial drops
022 on benchmarks requiring its specialized domain. (2) MiCRO’s behavior can be
023 dynamically steered at inference time by routing tokens to particular experts (e.g.,
024 favoring social over logical reasoning), enabling fine-grained control over out-
025 puts. (3) MiCRO outperforms or matches comparable baselines on both machine-
026 learning reasoning benchmarks (e.g., GSM8K, BBH) and alignment to human
027 behavior (CogBench), while maintaining interpretability. Taken together, cogni-
028 tively grounded functional specialization yields models that are both more human-
029 like and more human-interpretable.¹

030 1 INTRODUCTION

031 Neuroscience research suggests that distinct brain regions support language, reasoning, social cog-
032 nition, and other cognitive functions (Saxe & Kanwisher, 2003; Kanwisher, 2010; Fedorenko et al.,
033 2024). In contrast, the internal organization of Large Language Models (LLMs) is largely unstruc-
034 tured. While certain units or subnetworks show selective activation (Zhang et al., 2022; 2023;
035 Bayazit et al., 2023; AlKhamissi et al., 2025a; Wang et al., 2025), such specialization is implicit
036 and difficult to interpret or control. Motivated by this discrepancy, we propose a model architec-
037 ture that explicitly incorporates specialization. On the machine learning (ML) side, such designs
038 hold great potential for improving interpretability and controllability; on the cognitive science side,
039 they provide a framework toward formulating testable computational hypotheses about how the rel-
040 ative contributions of different brain networks support complex behavior. To this end, we propose
041 the Mixture of Cognitive Reasoners (MiCRO), a class of modular language models that partition
042 computation across brain-inspired expert modules.

043 The MiCRO architecture partitions each layer of a pretrained language model into four experts, each
044 designed to mirror a major cognitive network in the human brain: language (Fedorenko et al., 2011),
045 logic (multiple demand; Duncan, 2010), social reasoning (theory of mind; Saxe & Kanwisher, 2003),
046 and world knowledge (default mode; Gusnard et al., 2001). To provide the model with the inductive
047 bias needed to learn this partitioning and cohesively integrate these experts, we design a three-stage
048 curriculum that uses lightweight training in the first two stages to sequentially (1) specialize the
049 experts to mirror cognitive networks, and (2) bias a router to use certain experts for particular types
050 of inputs (e.g., the logic expert for mathematics problems). The final training stage of this curriculum
051 uses this now inductively-biased architecture to perform large-scale supervised finetuning.

052
053 ¹Code, data and models available at anonymous.4open.science/r/mixture-of-cognitive-reasoners-iclr

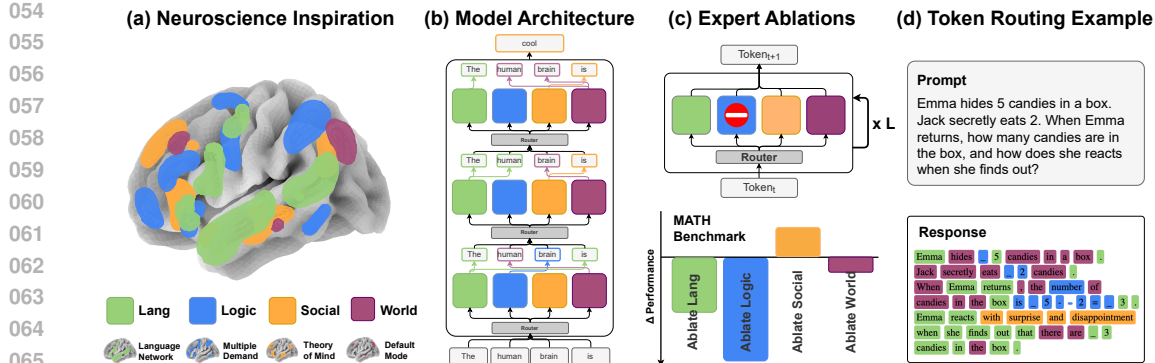


Figure 1: **Brain-Inspired Modular Language Model.** (a) Illustration of major cognitive networks in the human brain. (b) Our proposed Mixture of Cognitive Reasoners (MICRO) architecture. The MICRO architecture partitions each transformer block into four expert modules corresponding to analogous brain networks; a router assigns each token to an expert at every layer (i.e., assignments can vary across layers and tokens). (c) Illustration for causal steering via mechanistic ablations: removing a module shifts behavior and degrades domain-relevant performance. (d) Token-level routing on a sample prompt shows semantically coherent expert usage.

Our results demonstrate that MICRO’s architecture and training procedure induce interpretable specialization across these experts. This is evidenced by routing patterns and their correlations with human judgments (§5.1) and by causal ablations, which show dramatic drops in performance on reasoning categories when their corresponding experts are removed (§5.2). Moreover, the semantic behavior of these experts parallels the specialization of brain networks: (1) functional localizers used to recover brain-like mechanisms in LLMs (AlKhamissi et al., 2025a) identify the relevant experts in MICRO (§5.3), and (2) large MICRO models achieve high behavioral alignment scores on COGBENCH (Coda-Forno et al., 2024), a human behavioral benchmark, relative to two critical controls trained on the same data: (i) a mixture-of-experts model without induced brain-like specialization (MOB) and (ii) a non-modular dense transformer (DENSE) (§5.4). Finally, we find that MICRO’s performance matches or exceeds these baselines (§5.5), indicating that interpretable and controllable specialization can be achieved without sacrificing overall performance.

2 BACKGROUND & RELATED WORK

2.1 NEUROSCIENCE MOTIVATION

Our design follows evidence that human cognition emerges from interacting, specialized brain networks. Cognitive neuroscience has mapped this modular organization by measuring how strongly different regions engage when people perform specific cognitive tasks (Kanwisher, 2010). We align MICRO’s architecture with four core cognitive networks as shown in Figure 1(a). We summarize the functions of these networks below and their relevance to our modeling approach.

The Language Network. The *Language* expert mirrors the human language network, which comprises a set of left-lateralized frontal and temporal regions that selectively respond to linguistic input over perceptually matched non-linguistic stimuli (e.g., lists of nonwords; Fedorenko et al., 2010). These regions are highly specific to language, showing minimal activation during tasks such as arithmetic or music perception (Fedorenko et al., 2012; 2011), and their disruption can lead to selective language deficits (aphasia) without impairing general reasoning capabilities (Varley et al., 2005).

The Multiple Demand Network. The *Logic* expert mirrors the Multiple Demand (MD) network, which spans bilateral regions and is activated across diverse cognitively demanding tasks such as difficult math problems, with stronger responses for higher difficulty levels (Duncan & Owen, 2000; Fedorenko et al., 2013). It correlates with fluid intelligence (Woolgar et al., 2010).

108 **The Theory of Mind Network.** The *Social* expert mirrors the Theory of Mind (ToM) network,
 109 which is centered in the bilateral temporo-parietal junction and medial prefrontal cortex. This net-
 110 work supports reasoning about beliefs, intentions, and mental states (Gallagher et al., 2000; Saxe &
 111 Kanwisher, 2003; Saxe & Powell, 2006). It is robustly recruited across both verbal and non-verbal
 112 tasks involving perspective-taking and indirect communication (Koster-Hale & Saxe, 2013).

113
 114 **The Default Mode Network.** The *World* expert mirrors the Default Mode Network (DMN), which
 115 is active during rest and internally directed thought such as self-reflection, memory recall, and men-
 116 tal simulation (Gusnard et al., 2001; Buckner et al., 2008; Buckner & DiNicola, 2019). Centered in
 117 medial prefrontal and parietal regions, the DMN integrates information over long timescales, sup-
 118 porting discourse- and event-level processing across sentences or episodes (Hassabis & Maguire,
 119 2007; Fedorenko et al., 2024), in contrast to the shorter temporal scope of the language network.

120 2.2 MODULAR LANGUAGE MODELS

121
 122 In parallel with advances in cognitive neuroscience, recent years have seen growing interest in mod-
 123 ular language models as a way to promote specialization, mitigate interference, and improve out-of-
 124 distribution generalization (Pfeiffer et al., 2023; Zhang et al., 2025). One major line of work centers
 125 on Sparse Mixture-of-Experts (MoE) architectures (Shazeer et al., 2017), with approaches ranging
 126 from curating domain-labeled datasets to train (Gururangan et al., 2022) or prompt (Si et al., 2023)
 127 domain-specific experts, to frameworks such as ModuleFormer (Shen et al., 2023), which introduce
 128 load-balancing and concentration losses to encourage modular specialization without explicit do-
 129 main labels. Other modular approaches extend to multimodal integration (Liu et al., 2023; Swamy
 130 et al., 2023; Ye et al., 2023) or to disentangling representations by domain or language for multilin-
 131 gual and domain-specific applications (Pfeiffer et al., 2020; 2022; Zhong et al., 2022; Al-Maamari
 132 et al., 2024). In contrast, MiCRO is, to our knowledge, the first modular language model explicitly
 133 designed to induce brain-like specialization, aligning experts with well-studied cognitive networks.

134 2.3 BRAIN-INSPIRED MODELS

135
 136 Recent studies have shown that some models achieve strong alignment with activity in the human
 137 language network (Schrimpf et al., 2021; Toneva & Wehbe, 2019; Caucheteux & King, 2022; Aw
 138 et al., 2023; AlKhamissi et al., 2025b). To further improve brain alignment, researchers have begun
 139 to integrate biologically inspired principles into model design—drawing from structures like the
 140 visual cortex hierarchy (Kubilius et al., 2019; Dapello et al., 2020; Spoerer et al., 2020), and the
 141 spatio-functional organization of the brain (Margalit et al., 2024; Rathi et al., 2025).

142 3 THE MIXTURE OF COGNITIVE REASONERS FRAMEWORK

143 3.1 MODEL ARCHITECTURE

144
 145 To build MiCRO, we begin with a pretrained transformer-based backbone. For each layer, we
 146 clone the entire transformer block N times, where N corresponds to the number of experts intended
 147 for specialization, in a similar spirit to parameter upcycling (Komatsuzaki et al., 2023; Zhang et al.,
 148 2024). Then, we initialize a MLP-based router that assigns each token to a single expert. To maintain
 149 computational efficiency and a comparable number of active parameters to the original model, we
 150 use top-1 routing akin to Fedus et al. (2022). We refer to this architecture as *mixture-of-blocks*
 151 (MOB), distinguishing it from the more common mixture-of-experts (MOE), which restricts experts
 152 to FFN layers with shared attention. Importantly, we focus on MOB in the main paper because
 153 it induces clear functional specialization in all models, as reflected by lower router entropy and
 154 domain-consistent routing patterns, whereas MOE does not exhibit the same effect at specific scales
 155 (see Appendix H.1). Results for MiCRO-MOE variants on reasoning benchmarks in Appendix H.2.

156 3.2 TRAINING CURRICULUM FOR INDUCING SPECIALIZATION

157
 158 We induce functional specialization in MiCRO experts using a three-stage training curriculum (see
 159 Figure 2). The first two stages use a small, curated dataset (MiCRO_{SFT}) to provide targeted inductive
 160 biases, allowing specialization to emerge and solidify during the final full-scale training stage.

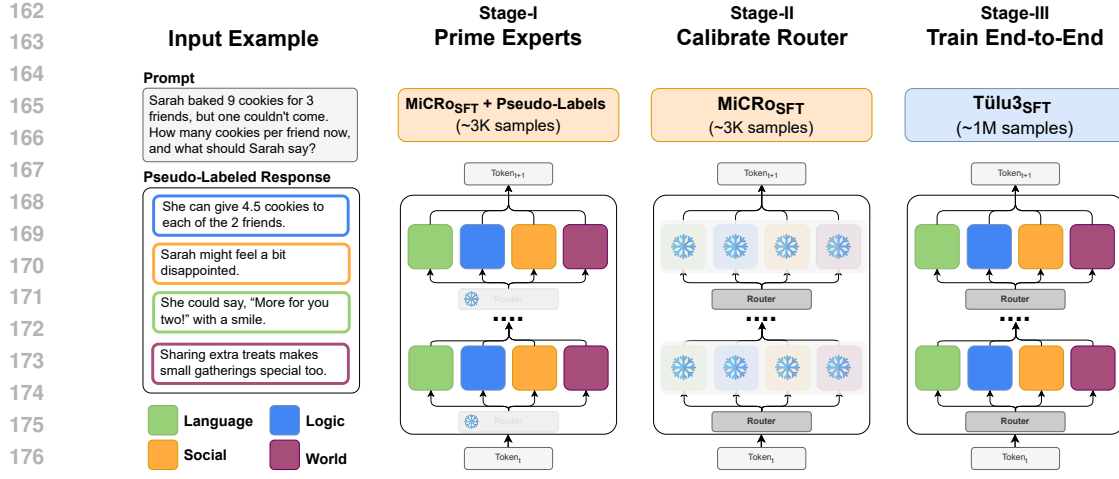


Figure 2: **Training Curriculum for Inducing Specialization.** Our brain-inspired Mixture of Cognitive Reasoners (MICRO) model contains four experts per layer, each aligned with a distinct cognitive network in the brain. In Stage-I, we train only the experts using a small, curated dataset MICROsFT (see example on the left), providing each expert with an initial inductive bias. In Stage-II, we freeze the whole model and train the router on the same dataset to learn expert selection. In Stage-III, we finetune the entire model end-to-end on a large-scale instruction tuning dataset.

Stage 1: Inducing Specialization. In the first stage, we train the experts on a small dataset of $M = 3055$ examples (described below), each crafted to reflect the functional domain of a specific expert (Section 2.1). We denote this dataset as $\text{MICROsFT} = \{(x_{i,1:T_i}, r_{i,1:T_i})\}_{i=1}^M$, where each input sequence x_i contains T_i tokens, and r_i provides token-level routing labels. Each label $r_{i,t} \in \{1, \dots, N\}$ assigns the t -th token to one of the N experts. This stage focuses solely on training the expert parameters using a next-token prediction loss. Tokens attend to all preceding tokens in the sequence regardless of which expert processed them using the key and value representations produced by the same expert. However, only tokens that are assigned to the expert in question continue to be processed through the feed-forward network. The same setup is applied in the next training stages, with the only difference that the router assigns the tokens to the experts.

Stage 2: Calibrating Router. Next, we freeze the whole model and train only the routers on the same dataset MICROsFT . The objective remains next-token prediction. Given the initial expert specialization from Stage 1, the router now learns to assign tokens to the most suitable expert. To encourage smoother transitions and more robust routing decisions, we use a soft mixture of the top-2 experts per token, which we found to be more effective than top-1 routing during this phase.

Stage 3: End-to-End Supervised Finetuning. Finally, we finetune the entire model end-to-end on a full instruction-tuning dataset, TÜLU-3 (Lambert et al., 2024), which consists of 939k examples. Even though this phase constitutes the majority of the training budget, we observe that the functional specialization seeded by the small MICROsFT dataset is largely preserved (see Appendix J). Moreover, the experts continue to improve on tasks aligned with their initial domains, demonstrating that early inductive biases can lead to meaningful and lasting functional decomposition.

Constructing the MICROsFT Dataset. To build MICROsFT for inducing expert and router specialization, we first selected 19 existing reasoning datasets corresponding to the cognitive domains of our non-language experts, ensuring that each group of datasets spanned a diverse range of functions known to engage the corresponding brain networks. From each of the three sets, we randomly sampled 1,000 examples and used OpenAI’s O1 model (Jaech et al., 2024) to generate detailed, step-by-step responses for each input. We then pseudo-labeled each sentence in the generated reasoning chains by prompting GPT-4O (Hurst et al., 2024) to assign it to one of the four experts. The tokens within each sentence inherit the corresponding expert label, which is used for deterministic routing in Stage 1. Details of the datasets are provided in Appendix A.

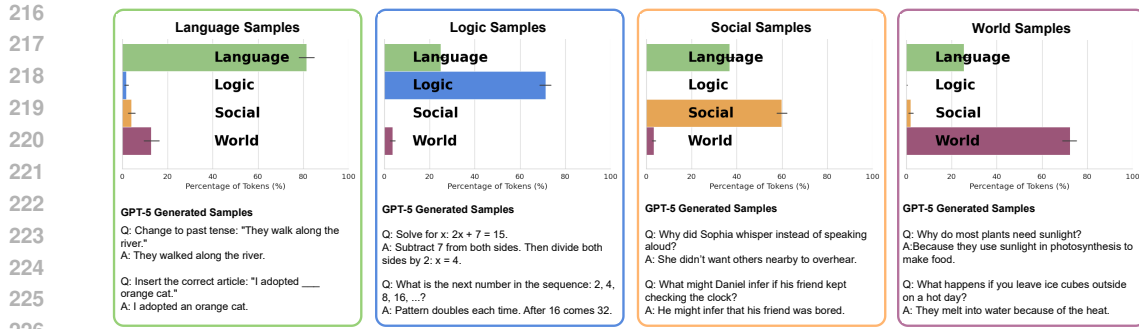


Figure 3: **Semantically Meaningful Routing Across Experts.** Token routing patterns in MICROLlama-1B. Each bar indicates the proportion of tokens routed to a given expert across layers, with variance shown across sentences ($n=50$). The model exhibits clear domain-specific specialization consistent with the intended brain-inspired organization. For example, social cognition samples are routed to the social expert, while arithmetic tasks are routed to the logic expert. We find that the language expert is consistently activated in the early layers (see Appendix C for layer-wise routing plots and results from additional models). Two random samples are shown below each subplot.

4 EXPERIMENTAL SETUP

We post-train five models of varying scales from three different families under our MICROLlama framework, in order to assess the generalizability of our method and identify the conditions under which it fails. Specifically, we use LLAMA-3.2-{1B, 3B} (Dubey et al., 2024), SMOLLM2-{135M, 360M} (Allal et al., 2025), and OLMO-2-1B (OLMO et al., 2024). Due to space constraints, we present the results of LLAMA-3.2-{1B, 3B} in the main paper while providing the full results for the remaining models in Appendix F. Each model is first finetuned for two epochs on the curated MICROLlamaSFT dataset (Stages 1 and 2), followed by one epoch of end-to-end training using the TÜLU-3 dataset (Lambert et al., 2024), as described in Section 3.2. We use next token prediction as the only learning objective in all training stages, with the loss masked on the input tokens. We use an effective batch size of 32 and the AdamW optimizer across all stages. The learning rate follows a linear schedule, warming up over the first 3% of training to a peak of 2×10^{-5} , then decays linearly for the remainder of training. This schedule is applied for each stage separately.

Reasoning Benchmarks. We evaluate on four widely used reasoning benchmarks: GSM8K (Cobbe et al., 2021), MATH (Hendrycks et al., 2021b), BBH (Suzgun et al., 2022), and MMLU (Hendrycks et al., 2021a). Evaluation follows zero- or fewshot settings as detailed in Appendix F.

Behavioral Benchmarks. We evaluate alignment to human behavior using COGBENCH benchmark (Coda-Forno et al., 2024), which provides 10 metrics from 7 cognitive psychology experiments. These metrics capture how participants (or models) complete tasks that are designed to disentangle different behavioral strategies. Examples include *Directed Exploration*, *Meta-Cognition*, and *Risk Taking*. We refer readers to Coda-Forno et al. (2024) for a detailed description of the tasks.

5 RESULTS & ANALYSIS

Our results unfold in two parts. First, we ask whether brain-like specialization emerges under our training curriculum, analyzing routing behavior, correlations with human judgments, causal ablations to test the functional contributions of those experts, and whether neuroscience experiments used to identify brain networks also identify the corresponding experts in our models. Second, we ask how this specialization influences alignment with human behavior and reasoning performance.

5.1 ROUTER PATTERNS ARE INTERPRETABLE AND CONSISTENT WITH HUMAN JUDGMENTS

Token Routing Per Expert. We first verify that our model routes tokens to the most relevant expert module, analogous to how specialized brain networks are selectively engaged by specific stim-

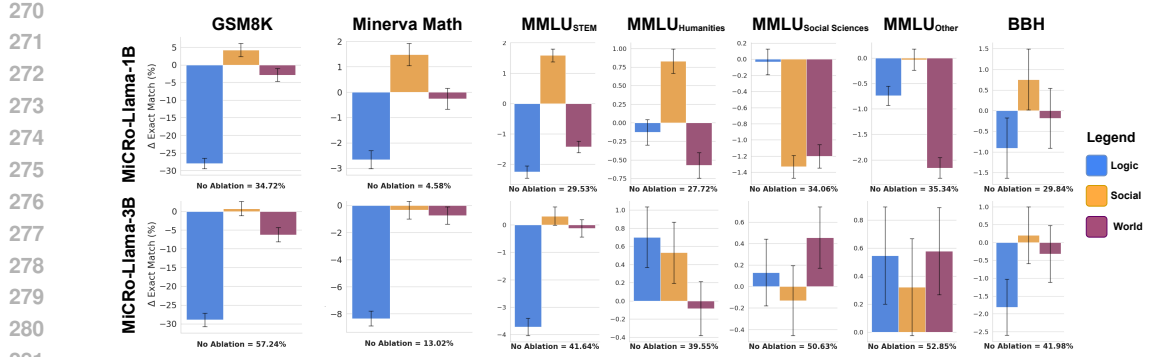


Figure 4: **Expert Ablations Reveal the Causal Contributions of Specialized modules.** Top and bottom panels show results for MICRo-LLAMA-1B and MICRo-LLAMA-3B. Removing the Logic expert causes large drops on MATH and GSM8K, while removing the Social expert yields slight gains. For MMLU and BBH, results indicate that some group of subtasks rely on distinct experts, whereas others draw on overlapping contributions. Additional models in Appendix E.

Figure 3 shows the routing behavior of MICRo-LLAMA-1B, revealing clear domain-specific specialization. To generate test inputs, we sampled 50 question–answer pairs using GPT-5 prompted with descriptions of the four brain networks (prompt provided in Appendix C). Results for the other MICRo variants are consistent and reported in Appendix C. There, we also show routing patterns on reasoning benchmarks, where tokens are directed to experts consistent with the benchmark’s domain. Finally, layer-wise analyses in Figures 13 & 14 reveal a hierarchical organization: earlier layers focus on linguistic grounding, while deeper layers increasingly delegate to domain-specific experts—an organization that emerged without being enforced by the training procedure and that parallels evidence from cognitive neuroscience (Fedorenko et al., 2024).

Correlation with Human Judgments. We evaluate model–human correspondence using 1,000 six-word sentences from Tuckute et al. (2024), each annotated with human ratings across several behavioral dimensions (e.g., mental state content, grammaticality). These annotations were collected independently of our routing framework. We find that router probabilities correlate with the corresponding human judgments: for example, the social expert’s selectivity aligns with ratings of mental state content ($r = 0.7$). Full results are provided in Appendix D.

5.2 EXPERTS ARE CAUSALLY MEANINGFUL

Validation of Functional Experts via Ablations. Figure 4 illustrates how expert ablations reveal the causal contributions of specialized modules to task performance. By selectively removing individual experts, we can directly test whether their specialization is functionally necessary for different domains. For example, on MATH and GSM8K, ablating the *Logic* expert causes a substantial drop in accuracy, confirming its central role in numerical reasoning. In contrast, removing the *Social* expert slightly improves performance, suggesting it plays a detrimental role in these tasks. For broader benchmarks such as MMLU, which span multiple subdomains, we report results for each subcategory separately. Performance drops after ablating the corresponding experts indicate that these clusters depend on distinct functional modules. Still, not all subtasks within a category align neatly with a single cognitive domain, and some require overlapping contributions, such as BBH. We show in Appendix E the effect of removing the language expert, which causes a significant drop on all benchmarks, along with additional ablation results on other models.

Steering Model Behavior at Test-Time. Our results demonstrate that test-time ablations can steer expert behavior, with social responses emerging when only the social expert is active and logical reasoning dominating when only the logic expert is retained. Qualitative examples in Appendix K.

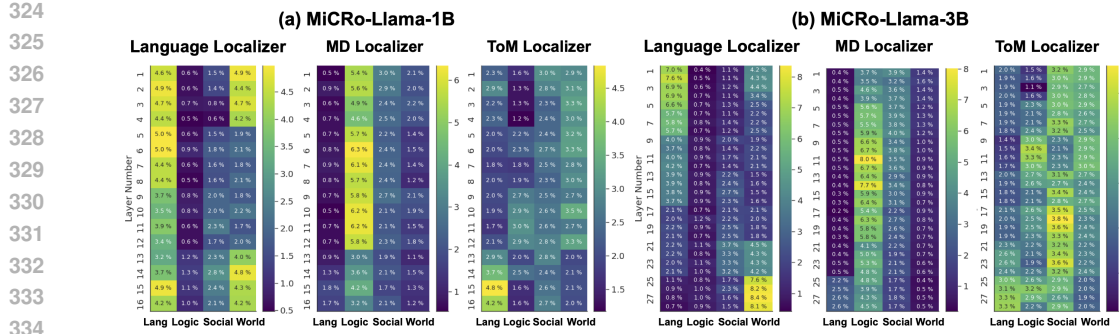


Figure 5: **Neuroscience Localizers Recover Functionally Specialized Experts.** (a) MiCRO-LLAMA-1B and (b) MiCRO-LLAMA-3B. For each model, we apply three neuroscience-inspired localizers—Language, Multiple Demand (MD) and Theory of Mind (ToM)—to examine the selectivity of localized units across experts and layers. Each plot shows the percentage of units in each expert of each layer that belongs to the top-10% selective units in the whole model.

5.3 NEUROSCIENCE LOCALIZERS REVEAL FUNCTIONAL EXPERT SPECIALIZATION

Neuroscientists rely on localizer experiments to identify the brain regions associated with specific functional networks, as their precise locations can vary across individuals. This raises a natural question: can we apply these established neuroscience localizers to identify the corresponding expert modules in our model? If so, this would provide further support for the hypothesis that our experts are functionally analogous to their associated brain networks.

To investigate this, we adopt the methodology of AlKhamissi et al. (2025a), which has been used to localize the language network, the multiple demand network, and the theory of mind network in LLMs. We apply these localizers to our MiCRO models to test whether they can recover the corresponding expert modules. Figure 5 shows the percentage of units in each expert of each layer that belongs to the top 10% of selective units across the whole model, similar to what is done in the brain (Lipkin et al., 2022). The results show that language selectivity, as defined by the language localizer, favors the language expert at early layers while favoring the world expert at later layers for both models. The multiple demand localizer successfully favors the logic expert in both models. In contrast, ToM localization is less effective at isolating units within the social experts, but improves with scale, suggesting that ToM ability must emerge before it can be localized. One other possible reason for this is the limited size of the ToM stimulus set, which includes only 10 contrastive pairs, in contrast to 240 for language and 100 for multiple demand. This small sample may lack the robustness needed to reliably localize ToM-selective units (Jamaa et al., 2025).

5.4 STRONG ALIGNMENT TO HUMAN BEHAVIOR

Having established that our MiCRO models exhibit human-like specialization (§5.1) that is causally linked to task performance (§5.2), we next examine whether they better align to human behavior compared to two baselines: one without brain-like specialization (MOB) and one without any modularization (DENSE). Both models are post-trained on a mixture of $2 \times$ MiCROsoft and $1 \times$ TÜLÜ-3 matching the total amount of data used in the MiCRO training curriculum.

Figure 6 presents the results on COGBENCH, evaluating alignment with human behavior. Unlike the original paper, which predicts answers via autoregressive generation, we pick the option with the highest log-probability for multiple-choice tasks to avoid invalid generations. Each experiment is run with five random seeds. Metrics are normalized such that random = 0 and human = 1. To quantify overall alignment, we introduce the bounded relative error similarity score (S_{BRE}), which avoids inflation from superhuman scores. For a normalized score s_i on metric i , we compute $BRE_i = |s_i - 1| / \max(1, s_i)$ and aggregate as $S_{BRE} = 1 - \frac{1}{n} \sum_{i=1}^n BRE_i$. Thus, BRE_i remains bounded in $[0, 1]$ even if $s_i > 1$.

Overall, we find competitive alignment across models, with MiCRO-LLAMA-1B showing superior alignment compared to its counterparts. Panel (a) reports the average similarity score (S_{BRE}) aggre-

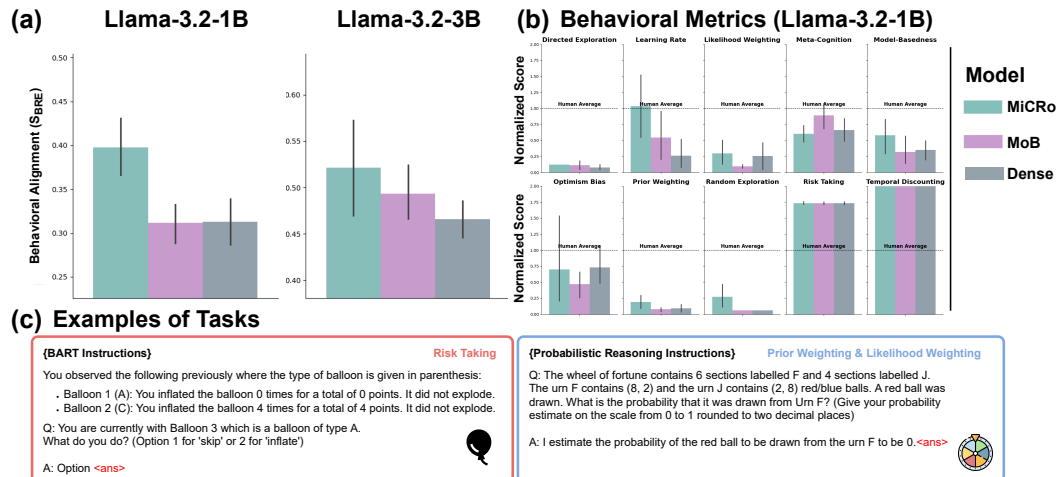


Figure 6: **Alignment with Human Behavior on COGBENCH.** (a) Average similarity score (S_{BRE}) across 10 behavioral metrics, showing that MiCRO-LLAMA models achieves superior alignment compared to their MoB and Dense baselines. (b) Human-normalized scores for each metric separately across the three models. (c) Example inputs from two of the seven classical psychological experiments verbalized for LLM evaluation following COGBENCH.

gated across the 10 behavioral metrics for both MiCRO-LLAMA-{1B, 3B} models, while panel (b) breaks down the human-normalized scores for each metric separately across the three post-trained models for the LLAMA-3.2-1B base model. Finally, panel (c) illustrates input examples from two of the seven classical psychological experiments included in COGBENCH, which are verbalized for LLM evaluation following the original benchmark design. More results in Appendix I.

5.5 COMPETITIVE PERFORMANCE ON REASONING BENCHMARKS

Here, we test whether our MiCRO models incur any performance degradation relative to their two baselines. Figure 7 shows performance on GSM8K, MINERVA-MATH, MMLU, MMLU-PRO, and BBH, along with their average. Models are evaluated using fewshot chain-of-thought prompting, except for GSM8K, which is evaluated under zero-shot CoT prompting. For both base models, MiCRO matches or exceeds comparable MoB baselines, while ablating the least relevant expert (i.e., the social expert for these benchmarks) further improves performance. We conduct pairwise Welch’s t -tests between models and report significance directly in the plot. Results show that some base models, such as LLAMA-3.2-1B, benefit significantly from brain-like specialization, whereas others, such as LLAMA-3.2-3B, only show significant differences relative to their baselines on some benchmarks. We report additional results for the other models and benchmarks in Appendix F. We further show that our method is robust to different post-training pipelines, including DPO (Rafailov et al., 2023) and domain-specific instruction tuning (Appendix G).

6 DISCUSSION & FUTURE WORK

Extending Specialization Beyond Cognitive Domains While inspired by the brain’s functional organization, our specialization framework can be applied to any meaningful partition of expertise, such as technical domains or natural languages. One key question is whether the model preserves the intended specialization through the large-scale end-to-end training. Our results suggest that brain-inspired partitions provide a robust inductive bias; they persist throughout training and lead to structured, interpretable routing patterns. Supporting evidence in Appendix J shows that expert usage remains consistent across checkpoints over the course of Stage 3 training. Looking ahead, this framework could also be extended to other cognitive domains. For example, recent neuroscience findings point to a distinct brain network involved in abstract formal reasoning such as induction

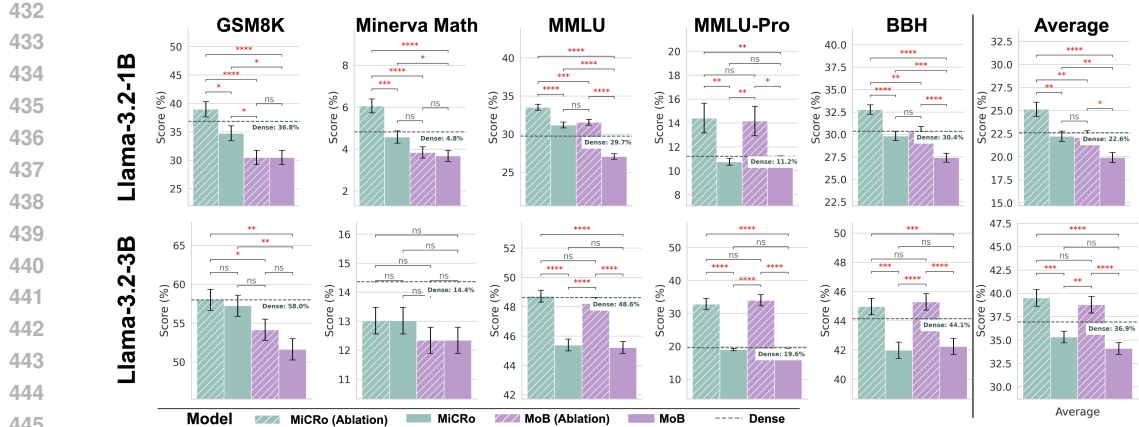


Figure 7: **Competitive Performance.** Results on GSM8K (0-shot CoT), MINERVA-MATH, MMLU, and BBH (fewshot CoT). MiCRO matches or outperforms baselines, and ablating the least relevant expert (e.g., social for math benchmarks) yields further gains. For MoB (ABLATION) and MiCRO (ABLATION) (on MMLU and BBH subtasks), results reflect the best performance obtained when ablating up to one expert. Significance is assessed with pairwise Welch’s t -tests (shown in plot; * denotes significant difference, while n.s. means not-significant). The dense model is shown as a dashed line. Results of the remaining models and on more benchmarks are provided in Appendix F.

and deduction and another network for intuitive physics (Kean et al., 2025a,b). Incorporating a corresponding module could improve the model’s performance on tasks involving such capacities.

The Crucial Role of Stage-1 Pretraining Data Our experiments highlight the importance of the curated MiCRO_{SFT} dataset in inducing effective specialization. Notably, we used only 3,055 samples in Stage-1, suggesting that even minimal domain-aligned supervision can shape expert behavior. This finding raises the possibility that different or more expansive data mixtures could further strengthen functional specialization and lead to additional gains in the model’s behavior.

Towards Brain Alignment Beyond Language Since our model is explicitly designed to mirror distinct cognitive networks in the human brain, and given that established neuroscience localizers can identify the corresponding expert modules, an exciting direction for future work is to examine whether the internal representations of these experts align more closely with neural activity in their respective brain networks (Schrimpf et al., 2018; 2020). Prior studies have shown that language-selective units in large language models correlate more strongly with activity in the human language network than randomly selected units (AlKhamissi et al., 2025a), suggesting a meaningful link between specialization in models and brains. This raises the natural question of whether similar alignment can be observed for other cognitive domains, such as reasoning or social cognition. However, assessing MiCRO’s neural alignment beyond the language network is currently limited by the lack of suitable datasets. Existing fMRI benchmarks rarely engage non-language regions such as the Multiple Demand (Duncan, 2010) network and often use blocked designs that preclude item-level analyses—highlighting the need for experimentalists to collect new datasets that explicitly target non-language brain regions. We believe that once suitable neural datasets exist, our model can be used to instantiate specific hypotheses about how these networks—and their corresponding experts—interact and exchange information.

Limitations While our approach improves interpretability without sacrificing performance, several open questions remain. Scaling beyond an 8B base model has yet to be demonstrated, and the impact of adding more experts to the current MiCRO architecture is still unknown. The MiCRO_{SFT} dataset used in Stage-1 (\approx 3,000 GPT-4o pseudo-labeled samples) has not been evaluated for size sensitivity, leaving open whether increasing or reducing its scale would alter the degree of specialization or downstream performance. Although GPT-4o provides high-quality pseudo-labels, as demonstrated in Appendix B, using human-annotated data could strengthen the inductive bias and

486 potentially improve the final model. We expect, however, that the potential of this approach will
 487 continue to grow as synthetic labellers become more accurate and reliable, enabling even stronger and
 488 more scalable specialization in future versions of this class of methods. Further, our post-training
 489 pipeline currently includes only SFT and DPO (Appendix G); exploring additional stages such as
 490 RLVR remains an avenue for future work. Finally, our evaluation of alignment to human behavior
 491 focuses on CogBench, and extending this analysis to a broader set of behavioral or cognitive datasets
 492 is an important direction for future research.

494 7 CONCLUSION

495
 496 This work presents the *Mixture of Cognitive Reasoners* (MiCRO), a modular architecture and train-
 497 ing paradigm inspired by the functional specialization of the human brain. By aligning expert mod-
 498 ules with distinct cognitive domains—language, logic, social reasoning, and world modeling—each
 499 reflecting the functionality of well-studied brain networks, we show that incorporating cognitive
 500 inductive biases into transformer models can effectively promote functional specialization. This re-
 501 sults in improved behavioral alignment as measured by COGBENCH, enhanced interpretability, all
 502 while being competitive or outperforming comparable models on reasoning benchmarks. Our staged
 503 training approach leverages a small curated dataset and enables specialization to emerge in a con-
 504 trollable and data-efficient manner. Furthermore, we show that the resulting modularity allows for
 505 targeted interventions at inference time, enabling the model to favor one mode of reasoning over an-
 506 other. These findings highlight a promising path toward more transparent, steerable, and cognitively
 507 grounded language models.

508 509 REFERENCES

510 Mohammed Al-Maamari, Mehdi Ben Amor, and Michael Granitzer. Mixture of modular ex-
 511 perts: Distilling knowledge from a multilingual teacher into specialized modular language
 512 models. *ArXiv*, abs/2407.19610, 2024. URL <https://api.semanticscholar.org/CorpusID:271533631>.

513
 514 Badr AlKhamissi, Greta Tuckute, Antoine Bosselut, and Martin Schrimpf. The LLM language
 515 network: A neuroscientific approach for identifying causally task-relevant units. In Luis
 516 Chiruzzo, Alan Ritter, and Lu Wang (eds.), *Proceedings of the 2025 Conference of the Na-
 517 tions of the Americas Chapter of the Association for Computational Linguistics: Human Lan-
 518 guage Technologies (Volume 1: Long Papers)*, pp. 10887–10911, Albuquerque, New Mex-
 519 ico, April 2025a. Association for Computational Linguistics. ISBN 979-8-89176-189-6. URL
 520 <https://aclanthology.org/2025.naacl-long.544/>.

521
 522 Badr AlKhamissi, Greta Tuckute, Yingtian Tang, Taha Binhraib, Antoine Bosselut, and Martin
 523 Schrimpf. From language to cognition: How llms outgrow the human language network. *arXiv
 524 preprint arXiv:2503.01830*, 2025b.

525
 526 Loubna Ben Allal, Anton Lozhkov, Elie Bakouch, Gabriel Martín Blázquez, Guilherme Penedo,
 527 Lewis Tunstall, Andrés Marafioti, Hynek Kydlíček, Agustín Piqueres Lajarín, Vaibhav Srivastav,
 528 et al. Smollm2: When smol goes big—data-centric training of a small language model. *arXiv
 529 preprint arXiv:2502.02737*, 2025.

530
 531 Khai Loong Aw, Syrielle Montariol, Badr AlKhamissi, Martin Schrimpf, and Antoine Bosselut.
 532 Instruction-tuning aligns llms to the human brain. 2023.

533
 534 Deniz Bayazit, Negar Foroutan, Zeming Chen, Gail Weiss, and Antoine Bosselut. Discovering
 535 knowledge-critical subnetworks in pretrained language models. *ArXiv*, abs/2310.03084, 2023.
 536 URL <https://api.semanticscholar.org/CorpusID:263671765>.

537
 538 Yonatan Bisk, Rowan Zellers, Ronan Le Bras, Jianfeng Gao, and Yejin Choi. Piqa: Reasoning
 539 about physical commonsense in natural language. In *Thirty-Fourth AAAI Conference on Artificial
 Intelligence*, 2020.

540
 541 Antoine Bosselut, Zeming Chen, Angelika Romanou, Antoine Bonnet, Alejandro Hernández-
 542 Cano, Badr AlKhamissi, Kyle Matoba, Francesco Salvi, Matteo Pagliardini, Simin Fan, Andreas

540 Köpf, Amirkeivan Mohtashami, Alexandre Sallinen, Vinitra Swamy, Alireza Sakhaeirad, Igor
 541 Krawczuk, Deniz Bayazit, Axel Marmet, Li Mi, and Martin Jaggi. Meditron: Open medical
 542 foundation models adapted for clinical practice, 03 2024.

543

544 Randy L. Buckner and Lauren M. DiNicola. The brain’s default network: updated anatomy,
 545 physiology and evolving insights. *Nature Reviews Neuroscience*, 20(10):593–608, September
 546 2019. ISSN 1471-0048. doi: 10.1038/s41583-019-0212-7. URL <http://dx.doi.org/10.1038/s41583-019-0212-7>.

547

548 Randy L. Buckner, Jessica R. Andrews-Hanna, and Daniel L. Schacter. The brain’s default network:
 549 Anatomy, function, and relevance to disease. *Annals of the New York Academy of Sciences*,
 550 1124(1):1–38, March 2008. ISSN 1749-6632. doi: 10.1196/annals.1440.011. URL <http://dx.doi.org/10.1196/annals.1440.011>.

551

552 Sven Buechel, Anneke Buffone, Barry Slaff, Lyle Ungar, and João Sedoc. Modeling empathy and
 553 distress in reaction to news stories. In Ellen Riloff, David Chiang, Julia Hockenmaier, and Jun’ichi
 554 Tsujii (eds.), *Proceedings of the 2018 Conference on Empirical Methods in Natural Language
 555 Processing*, pp. 4758–4765, Brussels, Belgium, October–November 2018. Association for Com-
 556 putational Linguistics. doi: 10.18653/v1/D18-1507. URL <https://aclanthology.org/D18-1507/>.

557

558 Charlotte Caucheteux and Jean-Rémi King. Brains and algorithms partially converge in natural
 559 language processing. *Communications biology*, 5(1):134, 2022.

560

561 Karl Cobbe, Vineet Kosaraju, Mohammad Bavarian, Mark Chen, Heewoo Jun, Lukasz Kaiser,
 562 Matthias Plappert, Jerry Tworek, Jacob Hilton, Reiichiro Nakano, Christopher Hesse, and John
 563 Schulman. Training verifiers to solve math word problems. *arXiv preprint arXiv:2110.14168*,
 564 2021.

565

566 Julian Coda-Forno, Marcel Binz, Jane X Wang, and Eric Schulz. CogBench: a large language
 567 model walks into a psychology lab. In Ruslan Salakhutdinov, Zico Kolter, Katherine Heller,
 568 Adrian Weller, Nuria Oliver, Jonathan Scarlett, and Felix Berkenkamp (eds.), *Proceedings of the
 569 41st International Conference on Machine Learning*, volume 235 of *Proceedings of Machine
 570 Learning Research*, pp. 9076–9108. PMLR, 21–27 Jul 2024. URL <https://proceedings.mlr.press/v235/coda-forno24a.html>.

571

572 Joel Dapello, Tiago Marques, Martin Schrimpf, Franziska Geiger, David D. Cox, and James J.
 573 DiCarlo. Simulating a Primary Visual Cortex at the Front of CNNs Improves Robustness to Image
 574 Perturbations. In *Neural Information Processing Systems (NeurIPS, Spotlight)*, June 2020. doi:
 575 10.1101/2020.06.16.154542. URL <https://www.biorxiv.org/content/10.1101/2020.06.16.154542v1>.

576

577 Abhimanyu Dubey, Abhinav Jauhri, Abhinav Pandey, Abhishek Kadian, Ahmad Al-Dahle, Aiesha
 578 Letman, and et al. The llama 3 herd of models. *ArXiv*, abs/2407.21783, 2024. URL <https://api.semanticscholar.org/CorpusID:271571434>.

579

580 John Duncan. The multiple-demand (md) system of the primate brain: mental programs for intelli-
 581 gent behaviour. *Trends in cognitive sciences*, 14(4):172–179, 2010.

582

583 John Duncan and Adrian M Owen. Common regions of the human frontal lobe recruited by
 584 diverse cognitive demands. *Trends in Neurosciences*, 23(10):475–483, October 2000. ISSN
 585 0166-2236. doi: 10.1016/s0166-2236(00)01633-7. URL [http://dx.doi.org/10.1016/S0166-2236\(00\)01633-7](http://dx.doi.org/10.1016/S0166-2236(00)01633-7).

586

587 Evelina Fedorenko, Po-Jang Hsieh, Alfonso Nieto-Castanon, Susan L. Whitfield-Gabrieli, and
 588 Nancy G. Kanwisher. New method for fmri investigations of language: defining rois func-
 589 tionally in individual subjects. *Journal of neurophysiology*, 104 2:1177–94, 2010. URL
 590 <https://api.semanticscholar.org/CorpusID:740913>.

591

592 Evelina Fedorenko, Michael K Behr, and Nancy Kanwisher. Functional specificity for high-level
 593 linguistic processing in the human brain. *Proceedings of the National Academy of Sciences*, 108
 (39):16428–16433, 2011.

594 Evelina Fedorenko, Josh H. McDermott, Sam Norman-Haignere, and Nancy Kanwisher. Sensitivity
 595 to musical structure in the human brain. *Journal of Neurophysiology*, 108(12):3289–3300, De-
 596 cember 2012. ISSN 1522-1598. doi: 10.1152/jn.00209.2012. URL <http://dx.doi.org/10.1152/jn.00209.2012>.

598 Evelina Fedorenko, John Duncan, and Nancy Kanwisher. Broad domain generality in focal re-
 599 gions of frontal and parietal cortex. *Proceedings of the National Academy of Sciences*, 110
 600 (41):16616–16621, September 2013. ISSN 1091-6490. doi: 10.1073/pnas.1315235110. URL
 601 <http://dx.doi.org/10.1073/pnas.1315235110>.

602 Evelina Fedorenko, Anna A. Ivanova, and Tamar I. Regev. The language network as a natural kind
 603 within the broader landscape of the human brain. *Nature Reviews Neuroscience*, 25(5):289–312,
 604 April 2024. ISSN 1471-0048. doi: 10.1038/s41583-024-00802-4. URL <http://dx.doi.org/10.1038/s41583-024-00802-4>.

605 William Fedus, Barret Zoph, and Noam Shazeer. Switch transformers: Scaling to trillion parameter
 606 models with simple and efficient sparsity. *Journal of Machine Learning Research*, 23(120):1–39,
 607 2022.

608 H.L Gallagher, F Happé, N Brunswick, P.C Fletcher, U Frith, and C.D Frith. Reading the mind in
 609 cartoons and stories: an fmri study of ‘theory of mind’ in verbal and nonverbal tasks. *Neuropsy-
 610 chologia*, 38(1):11–21, January 2000. ISSN 0028-3932. doi: 10.1016/s0028-3932(99)00053-6.
 611 URL [http://dx.doi.org/10.1016/s0028-3932\(99\)00053-6](http://dx.doi.org/10.1016/s0028-3932(99)00053-6).

612 Kanishk Gandhi, Jan-Philipp Fränken, Tobias Gerstenberg, and Noah Goodman. Understanding
 613 social reasoning in language models with language models. In *Thirty-seventh Conference on
 614 Neural Information Processing Systems Datasets and Benchmarks Track*, 2023. URL <https://openreview.net/forum?id=8bqjirgxQM>.

615 Leo Gao, Jonathan Tow, Baber Abbasi, Stella Biderman, Sid Black, Anthony DiPofi, Charles Fos-
 616 ter, Laurence Golding, Jeffrey Hsu, Alain Le Noac'h, Haonan Li, Kyle McDonell, Niklas Muen-
 617 nighoff, Chris Ociepa, Jason Phang, Laria Reynolds, Hailey Schoelkopf, Aviya Skowron, Lintang
 618 Sutawika, Eric Tang, Anish Thite, Ben Wang, Kevin Wang, and Andy Zou. The language model
 619 evaluation harness, 07 2024. URL <https://zenodo.org/records/12608602>.

620 Suchin Gururangan, Mike Lewis, Ari Holtzman, Noah A. Smith, and Luke Zettlemoyer. DEMix lay-
 621 ers: Disentangling domains for modular language modeling. In Marine Carpuat, Marie-Catherine
 622 de Marneffe, and Ivan Vladimir Meza Ruiz (eds.), *Proceedings of the 2022 Conference of the
 623 North American Chapter of the Association for Computational Linguistics: Human Language
 624 Technologies*, pp. 5557–5576, Seattle, United States, July 2022. Association for Computational
 625 Linguistics. doi: 10.18653/v1/2022.nacl-main.407. URL [https://aclanthology.org/2022.nacl-main.407/](https://aclanthology.org/2022.nacl-main.407).

626 Debra A. Gusnard, Erbil Akbudak, Gordon L. Shulman, and Marcus E. Raichle. Medial prefrontal
 627 cortex and self-referential mental activity: Relation to a default mode of brain function. *Pro-
 628 ceedings of the National Academy of Sciences*, 98(7):4259–4264, March 2001. ISSN 1091-6490. doi:
 629 10.1073/pnas.071043098. URL <http://dx.doi.org/10.1073/pnas.071043098>.

630 Simeng Han, Hailey Schoelkopf, Yilun Zhao, Zhenting Qi, Martin Riddell, Luke Benson, Lucy
 631 Sun, Ekaterina Zubova, Yujie Qiao, Matthew Burtell, David Peng, Jonathan Fan, Yixin Liu, Brian
 632 Wong, Malcolm Sailor, Ansong Ni, Linyong Nan, Jungo Kasai, Tao Yu, Rui Zhang, Shafiq Joty,
 633 Alexander R. Fabbri, Wojciech Kryscinski, Xi Victoria Lin, Caiming Xiong, and Dragomir Radev.
 634 Folio: Natural language reasoning with first-order logic. *arXiv preprint arXiv:2209.00840*, 2022.
 635 URL <https://arxiv.org/abs/2209.00840>.

636 Demis Hassabis and Eleanor A. Maguire. Deconstructing episodic memory with construction.
 637 *Trends in Cognitive Sciences*, 11(7):299–306, July 2007. ISSN 1364-6613. doi: 10.1016/j.tics.
 638 2007.05.001. URL <http://dx.doi.org/10.1016/j.tics.2007.05.001>.

639 Dan Hendrycks, Collin Burns, Steven Basart, Andy Zou, Mantas Mazeika, Dawn Song, and Ja-
 640 cob Steinhardt. Measuring massive multitask language understanding. In *International Confer-
 641 ence on Learning Representations*, 2021a. URL <https://openreview.net/forum?id=d7KBjmI3GmQ>.

648 Dan Hendrycks, Collin Burns, Saurav Kadavath, Akul Arora, Steven Basart, Eric Tang, Dawn Song,
 649 and Jacob Steinhardt. Measuring mathematical problem solving with the math dataset. *NeurIPS*,
 650 2021b.

651 Jennifer Hu, Sammy Floyd, Olessia Jouravlev, Evelina Fedorenko, and Edward Gibson. A fine-
 652 grained comparison of pragmatic language understanding in humans and language models. In
 653 Anna Rogers, Jordan Boyd-Graber, and Naoaki Okazaki (eds.), *Proceedings of the 61st Annual*
654 Meeting of the Association for Computational Linguistics (Volume 1: Long Papers), pp. 4194–
 655 4213, Toronto, Canada, July 2023. Association for Computational Linguistics. doi: 10.18653/v1/2023.acl-long.230. URL <https://aclanthology.org/2023.acl-long.230/>.

656 Aaron Hurst, Adam Lerer, Adam P Goucher, Adam Perelman, Aditya Ramesh, Aidan Clark, AJ Os-
 657 trow, Akila Welihinda, Alan Hayes, Alec Radford, et al. Gpt-4o system card. *arXiv preprint*
658 arXiv:2410.21276, 2024.

659 Hamish Ivison, Yizhong Wang, Jiacheng Liu, Ellen Wu, Valentina Pyatkin, Nathan Lambert, Yejin
 660 Choi, Noah A. Smith, and Hannaneh Hajishirzi. Unpacking dpo and ppo: Disentangling best
 661 practices for learning from preference feedback, 2024.

662 Aaron Jaech, Adam Kalai, Adam Lerer, Adam Richardson, Ahmed El-Kishky, Aiden Low, Alec
 663 Helyar, Aleksander Madry, Alex Beutel, Alex Carney, et al. Openai o1 system card. *arXiv*
664 preprint arXiv:2412.16720, 2024.

665 Yassine Jamaa, Badr AlKhamissi, Satrajit Ghosh, and Martin Schrimpf. Evaluating contrast local-
 666 izer for identifying causal units in social & mathematical tasks in language models. *arXiv preprint*
667 arXiv:2508.08276, 2025.

668 Nancy Kanwisher. Functional specificity in the human brain: A window into the functional archi-
 669 tecture of the mind. *Proceedings of the National Academy of Sciences*, 107(25):11163–11170,
 670 May 2010. ISSN 1091-6490. doi: 10.1073/pnas.1005062107. URL <http://dx.doi.org/10.1073/pnas.1005062107>.

671 Hope Kean, Alex Fung, Chiebuka Ohams, Jason Chen, Josh Rule, Joshua Tenenbaum, Steven Pi-
 672 antadosi, and Evelina Fedorenko. A human brain network specialized for abstract formal reason-
 673 ing. *bioRxiv*, 2025a. doi: 10.1101/2025.10.21.683445. URL <https://www.biorxiv.org/content/early/2025/10/21/2025.10.21.683445>.

674 Hope H. Kean, Alexander Fung, R.T. Pramod, Jessica Chomik-Morales, Nancy Kanwisher, and
 675 Evelina Fedorenko. Intuitive physical reasoning is not mediated by linguistic nor exclusively
 676 domain-general abstract representations. *Neuropsychologia*, 213:109125, July 2025b. ISSN
 677 0028-3932. doi: 10.1016/j.neuropsychologia.2025.109125. URL <http://dx.doi.org/10.1016/j.neuropsychologia.2025.109125>.

678 Hyunwoo Kim, Byeongchang Kim, and Gunhee Kim. Perspective-taking and pragmatics for gener-
 679 ating empathetic responses focused on emotion causes. In *EMNLP*, 2021.

680 Hyunwoo Kim, Melanie Sclar, Xuhui Zhou, Ronan Le Bras, Gunhee Kim, Yejin Choi, and Maarten
 681 Sap. Fantom: A benchmark for stress-testing machine theory of mind in interactions. In *EMNLP*,
 682 2023.

683 Aran Komatsuzaki, Joan Puigcerver, James Lee-Thorp, Carlos Riquelme Ruiz, Basil Mustafa,
 684 Joshua Ainslie, Yi Tay, Mostafa Dehghani, and Neil Houlsby. Sparse upcycling: Training
 685 mixture-of-experts from dense checkpoints. In *The Eleventh International Conference on Learn-
 686 ing Representations*, 2023. URL <https://openreview.net/forum?id=T5nUQDrM4u>.

687 Jorie Koster-Hale and Rebecca Saxe. Theory of mind: A neural prediction problem. *Neuron*,
 688 79(5):836–848, September 2013. ISSN 0896-6273. doi: 10.1016/j.neuron.2013.08.020. URL
 689 <http://dx.doi.org/10.1016/j.neuron.2013.08.020>.

690 Jonas Kubilius, Martin Schrimpf, Kohitij Kar, Ha Hong, Najib J Majaj, Rishi Rajalingham, Elias B
 691 Issa, Pouya Bashivan, Jonathan Prescott-Roy, Kailyn Schmidt, Aran Nayebi, Daniel Bear, Daniel
 692 L K Yamins, and James J DiCarlo. Brain-like object recognition with high-performing shallow
 693 recurrent anns. In *Advances in Neural Information Processing Systems*, 2019.

702 Nathan Lambert, Jacob Daniel Morrison, Valentina Pyatkin, Shengyi Huang, Hamish Ivison, Faeze
 703 Brahman, Lester James Validad Miranda, Alisa Liu, Nouha Dziri, Xinxi Lyu, Yuling Gu, Saumya
 704 Malik, Victoria Graf, Jena D. Hwang, Jiangjiang Yang, Ronan Le Bras, Oyvind Tafjord, Chris
 705 Wilhelm, Luca Soldaini, Noah A. Smith, Yizhong Wang, Pradeep Dasigi, and Hanna Hajishirzi.
 706 *Tülu 3: Pushing frontiers in open language model post-training.* *ArXiv*, abs/2411.15124, 2024.
 707 URL <https://api.semanticscholar.org/CorpusID:274192505>.

708 Guohao Li, Hasan Abed Al Kader Hammoud, Hani Itani, Dmitrii Khizbulin, and Bernard Ghanem.
 709 Camel: Communicative agents for "mind" exploration of large scale language model society,
 710 2023.

711 Lei Li, Yuanxin Liu, Linli Yao, Peiyuan Zhang, Chenxin An, Lean Wang, Xu Sun, Lingpeng Kong,
 712 and Qi Liu. Temporal reasoning transfer from text to video. In *The Thirteenth International
 713 Conference on Learning Representations*, 2025. URL <https://openreview.net/forum?id=sHAvMp5J4R>.

714 Benjamin Lipkin, Greta Tuckute, Josef Affourtit, Hannah Small, Zachary Mineroff, Hope Kean,
 715 Olessia Jouravlev, Lara Rakocevic, Brianna Pritchett, Matthew Siegelman, Caitlyn Hoeflin,
 716 Alvincé Pongos, Idan A. Blank, Melissa Kline Struhl, Anna Ivanova, Steven Shannon, Aalok
 717 Sathe, Malte Hoffmann, Alfonso Nieto-Castañón, and Evelina Fedorenko. Probabilistic atlases
 718 for the language network based on precision fmri data from 800 individuals. *Scientific
 719 Data*, 9(1), August 2022. ISSN 2052-4463. doi: 10.1038/s41597-022-01645-3. URL <http://dx.doi.org/10.1038/s41597-022-01645-3>.

720 Haotian Liu, Chunyuan Li, Qingyang Wu, and Yong Jae Lee. Visual instruction tuning, 2023.

721 Jian Liu, Leyang Cui, Hanmeng Liu, Dandan Huang, Yile Wang, and Yue Zhang. Logiqa: A
 722 challenge dataset for machine reading comprehension with logical reasoning. *arXiv preprint
 723 arXiv:2007.08124*, 2020.

724 Eshed Margalit, Hyodong Lee, Dawn Finzi, James J. DiCarlo, Kalanit Grill-Spector, and Daniel L.K.
 725 Yamins. A unifying framework for functional organization in early and higher ventral visual
 726 cortex. *Neuron*, 112(14):2435–2451.e7, July 2024. ISSN 0896-6273. doi: 10.1016/j.neuron.
 727 2024.04.018. URL <http://dx.doi.org/10.1016/j.neuron.2024.04.018>.

728 Team OLMo, Pete Walsh, Luca Soldaini, Dirk Groeneveld, Kyle Lo, Shane Arora, Akshita Bha-
 729 gia, Yuling Gu, Shengyi Huang, Matt Jordan, Nathan Lambert, Dustin Schwenk, Oyvind Tafjord,
 730 Taira Anderson, David Atkinson, Faeze Brahman, Christopher Clark, Pradeep Dasigi, Nouha
 731 Dziri, Michal Guerquin, Hamish Ivison, Pang Wei Koh, Jiacheng Liu, Saumya Malik, William
 732 Merrill, Lester James V. Miranda, Jacob Morrison, Tyler Murray, Crystal Nam, Valentina Py-
 733 atkin, Aman Rangapur, Michael Schmitz, Sam Skjonsberg, David Wadden, Christopher Wilhelm,
 734 Michael Wilson, Luke Zettlemoyer, Ali Farhadi, Noah A. Smith, and Hannaneh Hajishirzi. 2
 735 OLMo 2 Furious, 2024. URL <https://arxiv.org/abs/2501.00656>.

736 Jonas Pfeiffer, Ivan Vulić, Iryna Gurevych, and Sebastian Ruder. MAD-X: An Adapter-Based
 737 Framework for Multi-Task Cross-Lingual Transfer. In Bonnie Webber, Trevor Cohn, Yulan He,
 738 and Yang Liu (eds.), *Proceedings of the 2020 Conference on Empirical Methods in Natural Lan-
 739 guage Processing (EMNLP)*, pp. 7654–7673, Online, November 2020. Association for Computa-
 740 tional Linguistics. doi: 10.18653/v1/2020.emnlp-main.617. URL <https://aclanthology.org/2020.emnlp-main.617>.

741 Jonas Pfeiffer, Naman Goyal, Xi Lin, Xian Li, James Cross, Sebastian Riedel, and Mikel Artetxe.
 742 Lifting the curse of multilinguality by pre-training modular transformers. In Marine Carpuat,
 743 Marie-Catherine de Marneffe, and Ivan Vladimir Meza Ruiz (eds.), *Proceedings of the 2022
 744 Conference of the North American Chapter of the Association for Computational Linguistics:
 745 Human Language Technologies*, pp. 3479–3495, Seattle, United States, July 2022. Associa-
 746 tion for Computational Linguistics. doi: 10.18653/v1/2022.naacl-main.255. URL <https://aclanthology.org/2022.naacl-main.255>.

747 Jonas Pfeiffer, Sebastian Ruder, Ivan Vulić, and Edoardo Ponti. Modular deep learning. *Transactions
 748 on Machine Learning Research*, 2023. ISSN 2835-8856. URL <https://openreview.net/forum?id=z9EkXfvxta>. Survey Certification.

756 Yiwei Qin, Xuefeng Li, Haoyang Zou, Yixiu Liu, Shijie Xia, Zhen Huang, Yixin Ye, Weizhe Yuan,
 757 Zhengzhong Liu, Yuanzhi Li, and Pengfei Liu. O1 replication journey: A strategic progress report
 758 – part 1. <https://github.com/GAIR-NLP/O1-Journey>, 2024.

759

760 Rafael Rafailov, Archit Sharma, Eric Mitchell, Christopher D Manning, Stefano Ermon, and Chelsea
 761 Finn. Direct preference optimization: Your language model is secretly a reward model. In
 762 A. Oh, T. Naumann, A. Globerson, K. Saenko, M. Hardt, and S. Levine (eds.), *Advances in
 763 Neural Information Processing Systems*, volume 36, pp. 53728–53741. Curran Associates, Inc.,
 764 2023. URL https://proceedings.neurips.cc/paper_files/paper/2023/file/a85b405ed65c6477a4fe8302b5e06ce7-Paper-Conference.pdf.

765

766 Neil Rathi, Johannes Mehrer, Badr AlKhamissi, Taha Osama A Binhuraib, Nicholas Blauch, and
 767 Martin Schrimpf. TopoLM: brain-like spatio-functional organization in a topographic language
 768 model. In *The Thirteenth International Conference on Learning Representations*, 2025. URL
 769 <https://openreview.net/forum?id=aWXnKanInf>.

770 R Saxe and N Kanwisher. People thinking about thinking peoplethe role of the temporo-parietal
 771 junction in “theory of mind”. *NeuroImage*, 19(4):1835–1842, August 2003. ISSN 1053-
 772 8119. doi: 10.1016/s1053-8119(03)00230-1. URL [http://dx.doi.org/10.1016/s1053-8119\(03\)00230-1](http://dx.doi.org/10.1016/s1053-8119(03)00230-1).

773

774 Rebecca Saxe and Lindsey J. Powell. It’s the thought that counts: Specific brain regions for one
 775 component of theory of mind. *Psychological Science*, 17(8):692–699, August 2006. ISSN 1467-
 776 9280. doi: 10.1111/j.1467-9280.2006.01768.x. URL <http://dx.doi.org/10.1111/j.1467-9280.2006.01768.x>.

777

778 Martin Schrimpf, Jonas Kubilius, Ha Hong, Najib J. Majaj, Rishi Rajalingham, Elias B. Issa, Ko-
 779 hitij Kar, Pouya Bashivan, Jonathan Prescott-Roy, Franziska Geiger, Kailyn Schmidt, Daniel
 780 L. K. Yamins, and James J. DiCarlo. Brain-Score: Which Artificial Neural Network for Ob-
 781 ject Recognition is most Brain-Like? preprint, Neuroscience, September 2018. URL <https://biorxiv.org/lookup/doi/10.1101/407007>.

782

783

784 Martin Schrimpf, Jonas Kubilius, Michael J Lee, N Apurva Ratan Murty, Robert Ajemian, and
 785 James J DiCarlo. Integrative benchmarking to advance neurally mechanistic models of human
 786 intelligence. *Neuron*, 108(3):413–423, 2020.

787

788 Martin Schrimpf, Idan Asher Blank, Greta Tuckute, Carina Kauf, Eghbal A. Hosseini, Nancy
 789 Kanwisher, Joshua B. Tenenbaum, and Evelina Fedorenko. The neural architecture of lan-
 790 guage: Integrative modeling converges on predictive processing. *Proceedings of the National
 791 Academy of Sciences*, 118(45):e2105646118, 2021. doi: 10.1073/pnas.2105646118. URL
 792 <https://www.pnas.org/doi/abs/10.1073/pnas.2105646118>.

793

794 Noam Shazeer, *Azalia Mirhoseini, *Krzysztof Maziarz, Andy Davis, Quoc Le, Geoffrey Hin-
 795 ton, and Jeff Dean. Outrageously large neural networks: The sparsely-gated mixture-of-
 796 experts layer. In *International Conference on Learning Representations*, 2017. URL <https://openreview.net/forum?id=B1ckMDqlg>.

797

798 Yikang Shen, Zheyu Zhang, Tianyou Cao, Shawn Tan, Zhenfang Chen, and Chuang Gan. Mod-
 799 ulerformer: Modularity emerges from mixture-of-experts. 2023. URL <https://api.semanticscholar.org/CorpusID:261697418>.

800

801 Chenglei Si, Weijia Shi, Chen Zhao, Luke Zettlemoyer, and Jordan Boyd-Graber. Getting
 802 MoRE out of mixture of language model reasoning experts. In Houda Bouamor, Juan Pino,
 803 and Kalika Bali (eds.), *Findings of the Association for Computational Linguistics: EMNLP
 804 2023*, pp. 8234–8249, Singapore, December 2023. Association for Computational Linguistics.
 805 doi: 10.18653/v1/2023.findings-emnlp.552. URL <https://aclanthology.org/2023.findings-emnlp.552/>.

806

807 Courtney J. Spoerer, Tim C. Kietzmann, Johannes Mehrer, Ian Charest, and Nikolaus Kriegeskorte.
 808 Recurrent neural networks can explain flexible trading of speed and accuracy in biological
 809 vision. *PLOS Computational Biology*, 16(10):e1008215, October 2020. ISSN 1553-7358. doi:
 10.1371/journal.pcbi.1008215. URL <http://dx.doi.org/10.1371/journal.pcbi.1008215>.

810 Mirac Suzgun, Nathan Scales, Nathanael Schärlí, Sebastian Gehrmann, Yi Tay, Hyung Won Chung,
 811 Aakanksha Chowdhery, Quoc V Le, Ed H Chi, Denny Zhou, , and Jason Wei. Challenging big-
 812 bench tasks and whether chain-of-thought can solve them. *arXiv preprint arXiv:2210.09261*,
 813 2022.

814 Vinitra Swamy, Malika Satayeva, Jibril Frej, Thierry Bossy, Thijs Vogels, Martin Jaggi, Tanja Käser,
 815 and Mary-Anne Hartley. MultimoDN—multimodal, multi-task, interpretable modular networks.
 816 In *Thirty-seventh Conference on Neural Information Processing Systems*, 2023. URL <https://openreview.net/forum?id=iB3Ew6z4WL>.

817

818 Mariya Toneva and Leila Wehbe. Interpreting and improving natural-language processing (in ma-
 819 chines) with natural language-processing (in the brain). In *Neural Information Processing Sys-
 820 tems*, 2019. URL <https://api.semanticscholar.org/CorpusID:167217728>.

821

822 Greta Tuckute, Aalok Sathe, Shashank Srikant, Maya Taliaferro, Mingye Wang, Martin Schrimpf,
 823 Kendrick Kay, and Evelina Fedorenko. Driving and suppressing the human language network
 824 using large language models. *Nature Human Behaviour*, pp. 1–18, 2024.

825

826 Rosemary A. Varley, Nicolai J. C. Klessinger, Charles A. J. Romanowski, and Michael Sie-
 827 gal. Agrammatic but numerate. *Proceedings of the National Academy of Sciences*, 102(9):
 828 3519–3524, February 2005. ISSN 1091-6490. doi: 10.1073/pnas.0407470102. URL <http://dx.doi.org/10.1073/pnas.0407470102>.

829

830 Chengcheng Wang, Zhiyu Fan, Zaizhu Han, Yanchao Bi, and Jixing Li. Emergent modularity
 831 in large language models: Insights from aphasia simulations. *bioRxiv*, 2025. doi: 10.1101/
 832 2025.02.22.639416. URL <https://www.biorxiv.org/content/early/2025/02/23/2025.02.22.639416>.

833

834

835 Jiayu Wang, Yifei Ming, Zhenmei Shi, Vibhav Vineet, Xin Wang, Yixuan Li, and Neel Joshi. Is a
 836 picture worth a thousand words? delving into spatial reasoning for vision language models. In
 837 *The Thirty-Eighth Annual Conference on Neural Information Processing Systems*, 2024.

838

839 Yizhong Wang, Swaroop Mishra, Pegah Alipoormolabashi, Yeganeh Kordi, Amirreza Mirzaei, An-
 840 jana Arunkumar, Arjun Ashok, Arut Selvan Dhanasekaran, Atharva Naik, David Stap, Eshaan
 841 Pathak, Giannis Karamanolakis, Haizhi Gary Lai, Ishan Purohit, Ishani Mondal, Jacob Anderson,
 842 Kirby Kuznia, Krima Doshi, Maitreya Patel, Kuntal Kumar Pal, Mehrad Moradshahi, Mihir Par-
 843 mar, Mirali Purohit, Neeraj Varshney, Phani Rohitha Kaza, Pulkit Verma, Ravsehaj Singh Puri,
 844 Rushang Karia, Shailaja Keyur Sampat, Savan Doshi, Siddhartha Mishra, Sujan Reddy, Sumanta
 845 Patro, Tanay Dixit, Xudong Shen, Chitta Baral, Yejin Choi, Noah A. Smith, Hannaneh Hajishirzi,
 846 and Daniel Khashabi. Super-naturalinstructions: Generalization via declarative instructions on
 847 1600+ nlp tasks, 2022. URL <https://arxiv.org/abs/2204.07705>.

848

849 Alexandra Woolgar, Alice Parr, Rhodri Cusack, Russell Thompson, Ian Nimmo-Smith, Teresa Tor-
 850 ralva, Maria Roca, Nagui Antoun, Facundo Manes, and John Duncan. Fluid intelligence loss
 851 linked to restricted regions of damage within frontal and parietal cortex. *Proceedings of the
 852 National Academy of Sciences*, 107(33):14899–14902, August 2010. ISSN 1091-6490. doi:
 853 10.1073/pnas.1007928107. URL <http://dx.doi.org/10.1073/pnas.1007928107>.

854

855 Yi Yang, Wen-tau Yih, and Christopher Meek. WikiQA: A challenge dataset for open-domain
 856 question answering. In *Proceedings of the 2015 Conference on Empirical Methods in Natural
 857 Language Processing*, pp. 2013–2018, Lisbon, Portugal, September 2015. Association for Com-
 858 putational Linguistics. doi: 10.18653/v1/D15-1237. URL <https://aclanthology.org/D15-1237>.

859

860 Qinghao Ye, Haiyang Xu, Jiabo Ye, Ming Yan, Anwen Hu, Haowei Liu, Qi Qian, Ji Zhang, Fei
 861 Huang, and Jingren Zhou. mplug-owl2: Revolutionizing multi-modal large language model with
 862 modality collaboration, 2023.

863

864 Danyang Zhang, Junhao Song, Ziqian Bi, Yingfang Yuan, Tianyang Wang, Joe Yeong, and Junfeng
 865 Hao. Mixture of experts in large language models. *ArXiv*, abs/2507.11181, 2025. URL <https://api.semanticscholar.org/CorpusID:280277258>.

864 Qizhen Zhang, Nikolas Gritsch, Dwaraknath Gnaneshwar, Simon Guo, David Cairuz, Bharat
 865 Venkitesh, Jakob Nicolaus Foerster, Phil Blunsom, Sebastian Ruder, Ahmet Üstün, and Acyr
 866 Locatelli. BAM! just like that: Simple and efficient parameter upcycling for mixture of experts.
 867 In *The Thirty-eighth Annual Conference on Neural Information Processing Systems*, 2024. URL
 868 <https://openreview.net/forum?id=BDrWQTrfyI>.

869 Zhengyan Zhang, Yankai Lin, Zhiyuan Liu, Peng Li, Maosong Sun, and Jie Zhou. MoEfica-
 870 tion: Transformer feed-forward layers are mixtures of experts. In Smaranda Muresan, Preslav
 871 Nakov, and Aline Villavicencio (eds.), *Findings of the Association for Computational Linguistics:*
 872 *ACL 2022*, pp. 877–890, Dublin, Ireland, May 2022. Association for Computational Linguis-
 873 tics. doi: 10.18653/v1/2022.findings-acl.71. URL <https://aclanthology.org/2022.findings-acl.71/>.

874 Zhengyan Zhang, Zhiyuan Zeng, Yankai Lin, Chaojun Xiao, Xiaozhi Wang, Xu Han, Zhiyuan
 875 Liu, Ruobing Xie, Maosong Sun, and Jie Zhou. Emergent modularity in pre-trained trans-
 876 formers. In Anna Rogers, Jordan Boyd-Graber, and Naoaki Okazaki (eds.), *Findings of the*
 877 *Association for Computational Linguistics: ACL 2023*, pp. 4066–4083, Toronto, Canada, July
 878 2023. Association for Computational Linguistics. doi: 10.18653/v1/2023.findings-acl.250. URL
 879 <https://aclanthology.org/2023.findings-acl.250/>.

880 Tao Zhong, Zhixiang Chi, Li Gu, Yang Wang, Yuanhao Yu, and Jin Tang. Meta-DMoe: Adapting to
 881 domain shift by meta-distillation from mixture-of-experts. In *Thirty-Sixth Conference on Neural*
 882 *Information Processing Systems (NeurIPS)*, 2022.

883
 884
 885
 886
 887
 888
 889
 890
 891
 892
 893
 894
 895
 896
 897
 898
 899
 900
 901
 902
 903
 904
 905
 906
 907
 908
 909
 910
 911
 912
 913
 914
 915
 916
 917

APPENDIX

A CONSTRUCTING THE EXPERTS DATASET

Datasets To construct the small curated datasets used in stages 1 and 2 of our training curriculum, we first identified existing datasets that align with the cognitive domain of each expert. Table 1 lists these datasets, the number of examples sampled from each, the corresponding high-level cognitive skill they were chosen to represent, and whether we used O1 to generate responses or relied on the original reasoning chains provided with the dataset.

Table 1: **Datasets Used to Induce Specialization in Stage-1.** Overview of datasets used to induce expert specialization during stages 1 and 2. Each dataset is aligned with a cognitive skill targeted by a specific expert. We indicate the number of examples sampled from each dataset and whether responses were generated using O1 or taken directly from the dataset’s original reasoning chains.

Expert	Task	Dataset	# Samples	Use O1
Logic	Math	O1-Journey (Qin et al., 2024)	327	No
		Math (Li et al., 2023)	200	No
		GSM8K (Cobbe et al., 2021)	100	Yes
	Logic	Folio (Han et al., 2022)	100	Yes
		LogicQA (Liu et al., 2020)	100	Yes
	Physics	Physics (Li et al., 2023)	200	No
Total (Logic)			1027	
Social	Pragmatics	Deceits (Hu et al., 2023)	20	Yes
		Indirect Speech (Hu et al., 2023)	20	Yes
		Irony (Hu et al., 2023)	25	Yes
		Maxims (Hu et al., 2023)	19	Yes
		Metaphor (Hu et al., 2023)	20	Yes
		Humor (Hu et al., 2023)	25	Yes
	Emotion Detection	Coherence (Hu et al., 2023)	40	Yes
		EmoCause (Kim et al., 2021)	100	Yes
		FanToM 1st Order (Kim et al., 2023)	100	Yes
	Theory of Mind	FanToM 2nd Order (Kim et al., 2023)	100	Yes
		BigToM (Gandhi et al., 2023)	128	Yes
	Social Reasoning	Mixture ProlificAI/social-reasoning-rlhf	531	Yes
Total (Social)			1028	
World	World Knowledge	Biology (Li et al., 2023)	100	No
		Chemistry (Li et al., 2023)	100	No
		PIQA (Bisk et al., 2020)	200	Yes
		WikiQA (Yang et al., 2015)	100	Yes
	Spatial Reasoning	SpatialEval (Wang et al., 2024)	100	Yes
	Temporal Reasoning	TextTemporal (Li et al., 2025)	100	Yes
	World Building	World Building archit11/worldbuilding	200	No
	Cause Effect	CoPA (Wang et al., 2022)	100	Yes
	Total (World)			1000

Generating Reasoning Responses Since most of the existing datasets we identified (listed in Table 1) do not include reasoning steps for the final answer, we used O1 to generate them. Specifically, we prompted the model with the input followed by “Let’s think step by step.” to elicit a longer response that includes intermediate reasoning before reaching the final answer. This was only done for datasets that did not already contain suitable reasoning chains.

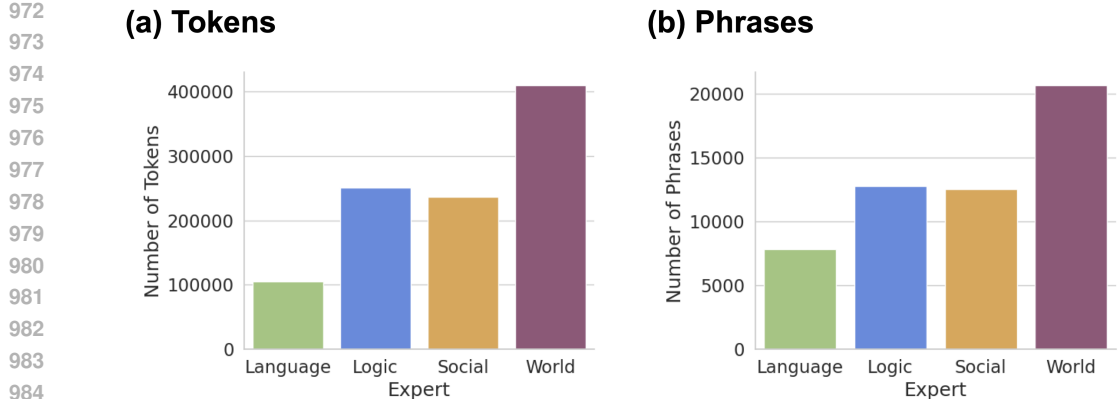


Figure 8: **Distribution of Expert Assignments across Tokens and Phrases.** (a) The distribution of expert assignments across tokens using the LLAMA-3.2-1B tokenizer. (b) The distribution of expert assignments labeled using GPT-4O for each phrase in the provided response.

Pseudo-Labeling Responses Finally, once we obtained responses with intermediate reasoning steps for all sampled examples, we used GPT-4O to pseudo-label each phrase in the response. During stage-1 training, each token in a phrase was then assigned to the expert identified by the pseudo-label. This labeling process was guided by the prompt shown in Figure 9. Figure 11 provides examples of labeled responses, while Figure 8 shows the distribution of expert assignments across tokens and phrases.

B INTER-ANNOTATOR AGREEMENT ANALYSIS OF $\text{MICRO}_{\text{SFT}}$

We assess the reliability of the $\text{MICRO}_{\text{SFT}}$ pseudo-labels using a set of standard agreement metrics between three human annotators and the GPT-4O labels on a subset of the $\text{MICRO}_{\text{SFT}}$ dataset. For the three human annotators, we report Krippendorff's α (a chance-corrected multi-annotator reliability metric), Fleiss' κ (multi-rater extension of Cohen's κ), and pairwise Cohen's κ with percent agreement. We also measure the agreement between the humans and the LLM labels both against the human majority vote and by treating the LLM as a fourth annotator.

B.1 HUMAN–HUMAN AGREEMENT

Table 2 summarizes agreement across the three human annotators. Both Krippendorff's α and Fleiss' κ indicate moderate reliability (0.517). The three-way exact agreement rate (all annotators assign the same label) is 49.4%.

Pairwise metrics (Table 3) reveal that annotators H1 and H2 exhibit stronger mutual agreement ($\kappa = 0.681$) relative to H1–H3 and H2–H3, which show lower yet nontrivial agreement levels ($\kappa \approx 0.43\text{--}0.45$).

Table 2: Agreement among human annotators.

Metric	Value
Krippendorff's α (nominal, 3 annotators)	0.517
Fleiss' κ (3 annotators)	0.517
3-way exact agreement	49.4%

B.2 HUMAN–LLM AGREEMENT

We evaluate human–LLM agreement in two ways: (1) comparing the LLM to the majority-vote label of the three humans, and (2) treating the LLM as a fourth annotator.

1026
 1027
 1028
 1029
GPT-4o Prompt for Pseudo-labeling O1 Responses
 1030
 1031 I am training a mixture-of-experts (MoE) model that routes tokens individually (token-level routing) to specialized experts. The
 1032 model includes four distinct experts, each clearly analogous to a specific cognitive network in the human brain. Below is a detailed
 1033 explanation of each expert, along with examples of the types of tasks or token sequences each should typically handle:
 1034
 - **Language Network (LN):** Primarily responsible for linguistic processing, grammatical structures, vocabulary usage, syntax,
 1035 semantics, and sentence coherence. This expert should handle tasks involving language comprehension, text fluency, sentence
 1036 construction, paraphrasing, and interpreting linguistic nuances.
 - Example tasks: Completing sentences, grammar correction, paraphrasing sentences, translating between languages,
 summarizing text.
 1037
 - **Multiple Demand Network (MD):** Specializes in analytical thinking, mathematical calculations, numerical reasoning, and logical
 1038 problem-solving. This expert engages explicitly in arithmetic operations, logical deductions, comparisons, quantitative reasoning,
 and systematic analysis.
 - Example tasks: Performing arithmetic operations, solving logical puzzles, analyzing numerical data, interpreting
 1039 mathematical expressions, evaluating logical arguments.
 1040
 - **Theory of Mind Network (ToM):** Dedicated to social cognition and interpersonal reasoning. This expert interprets and predicts
 1041 social interactions, emotional states, intentions, desires, beliefs, and motivations of individuals or groups.
 - Example tasks: Inferring a person's feelings or intentions from their actions, understanding dialogue involving interpersonal
 1042 relations, predicting characters' behaviors based on emotional context, interpreting subtle social cues.
 1043
 - **Default Mode Network (DMN):** Responsible for integrating general world knowledge, context understanding, background
 1044 information retrieval, and conceptual reasoning about everyday scenarios or common-sense understanding.
 - Example tasks: Providing background knowledge on common scenarios, contextualizing real-world situations, recalling
 1045 general facts, understanding cause-and-effect relationships, providing narrative context.
 1046
 1047 Given the following example of model-generated text in response to a prompt, carefully label each token sequence with the expert
 1048 best suited to handle it (LN, MD, ToM, or DMN). Ensure each sequence is assigned to only one expert. Output your answer clearly
 and explicitly in the following JSON format with each {sequence_i} corresponding to the actual sequence of tokens:
 1049
 1050 ```json
 1051 {
 1052 "sequence_1": "{expert_label}",
 1053 "sequence_2": "{expert_label}",
 1054 "sequence_3": "{expert_label}",
 1055 ...
 1056 }
 1057
 1058 ## Prompt
 1059 {prompt}
 1060
 1061 ## Generation
 1062 {generation}

1062 **Figure 9: Prompt Used for Pseudo-Labeling O1 Responses** The prompt used to instruct GPT-4o
 1063 to label the O1 model generations given a specific input prompt.
 1064

1065
 1066
 1067
 1068
GPT-5 Prompt for Generating Expert Specific Stimuli
 1069
 1070 {BRAIN_NETWORKS_DESCRIPTION}
 1071
 1072 Using the description above and your knowledge of the mentioned brain networks, generate {N} prompt and chain of thought
 1073 answer pairs that activate only the {BRAIN_NETWORK} expert and do not activate any of the other experts. Output the results only
 1074 and nothing else in JSONL format. Each JSON object should be in an LLM chat format as the following.
 1075
 1076 ...
 1077 {"user": <prompt>, "assistant": <cot-answer>}

1076 **Figure 10: Expert-Specific Prompt Template Used with GPT-5** Prompt provided to GPT-5
 1077 for generating expert-specific question-answer pairs. The stimuli for each expert was prompted
 1078 separately using the same brain-network descriptions as in Figure 9.
 1079

1080

1081

1082

1083

1084

1085

1086

1087

1088

1089

(a)

Input Prompt

Task: You will read pairs of sentences. Reach each pair and decide whether they form a coherent story. The answer options are 1 or 2.

Scenario: Mary's exam was about to start. Her palms were sweaty.
Options:
1) Incoherent
2) Coherent
Let's think step by step:

1097

Response

- Step 1: Read the sentences carefully.
- Sentence 1: "Mary's exam was about to start."
- Sentence 2: "Her palms were sweaty."
- Step 2: Analyze the logical connection between the sentences.
 - The first sentence introduces a situation where Mary is about to take an exam.
 - The second sentence describes a physical reaction (sweaty palms) that is commonly associated with nervousness or anxiety.
 - Nervousness is a typical emotion before an exam.
- Step 3: Determine if the sentences form a coherent story.
 - The physical reaction in the second sentence logically follows the situation in the first sentence.
 - There is a clear cause (exam starting) and effect (sweaty palms due to nervousness).
- **Answer:** 2) Coherent

1098

1099

1100

1101

1102

1103

1104

1105

1106

1107

1108

1109

1110

1111

1112

1113

1114

1115

1116

1117

Expert Legend**Language****Logic****Social****World**

1118

1119

1120

1121

1122

1123

1124

1125

1126

1127

1128

1129

1130

1131

1132

1133

(b)

Input Prompt

A cube with an edge length of 4 units has the same volume as a square-based pyramid with base edge lengths of 8 units and a height of $\$h\$$ units. What is the value of $\$h\$$?

Response

- Let's work through this problem step by step, keeping a close eye on each detail and exploring any uncertainties as we go. Our goal is to find the height $\|(h \|)$ of a square-based pyramid given that its volume matches that of a cube with an edge length of 4 units.
- To start, we know the volume of a cube is given by the formula $\| V_{\text{cube}} \| = s^3$. With $\|(s = 4 \|)$, we calculate the volume of the cube:
- $\| V_{\text{cube}} \| = 4^3 = 64$
- Now, let's consider the pyramid. The volume of a square-based pyramid is determined by the formula $\| V_{\text{pyramid}} \| = \frac{1}{3} \times \text{base area} \times \text{height}$. The base area for our pyramid, given the base edge length $\|(l = 8 \|)$, is $\| 8^2 \|$.
- Substituting into the formula, we have:
- ...
- So, it appears the height $\|(h \|)$ is 3 units. Let's pause and consider what we have done so far. Initially, we encountered a mistake with division, but after revisiting our steps, we corrected it by accurately isolating $\|(h \|)$.
- Thus, the final height $\|(h \|)$ of the pyramid, maintaining the equality of volumes, is $\| \boxed{3} \|$.

Figure 11: **Examples of Pseudo-Labeled Responses using GPT-4O** (a) shows a response generated by O1 for a prompt from the coherence subset of the PRAGMATICS dataset (Hu et al., 2023). (b) shows a response taken directly from the O1-JOURNEY dataset (Qin et al., 2024). Each subfigure includes the original prompt, the full model-generated response, and the corresponding pseudo-labels assigned to each phrase.

1134
1135
1136
1137
1138
1139
1140
1141

1142 Table 3: Pairwise agreement between human annotators.

Annotator Pair	Percent Agreement	Cohen's κ
H1–H2	76.3%	0.681
H1–H3	58.9%	0.431
H2–H3	58.5%	0.446

1144
1145
1146
1147

LLM vs. Human Majority Vote. Out of the full set, 240 items had a unique human majority label (13 items exhibited three-way ties). On this subset, the LLM achieves the performance shown in Table 4. The Cohen's κ between the LLM and the majority vote is 0.533, indicating substantial agreement comparable to human–human levels.

1148
1149
1150
1151
1152
1153
1154
1155
1156
1157
1158
1159
1160
1161
1162
1163
1164
1165
1166
1167
1168
1169
1170
1171
1172
1173
1174
1175
1176
1177
1178
1179
1180
1181
1182
1183
1184
1185
1186
1187

Table 4: LLM agreement with human majority-vote labels.

Metric	Value
Accuracy	0.658
Macro F1	0.666
Cohen's κ (LLM vs. majority)	0.533

LLM as a Fourth Annotator. We also compute multi-annotator reliability including the LLM (Table 5). Krippendorff's α decreases slightly to 0.497, reflecting the LLM's moderate alignment with the human annotators.

Pairwise comparisons between each human annotator and the LLM (Table 6) show agreement levels similar to those between some human pairs (particularly H1–H3 and H2–H3).

Table 5: Agreement among 3 humans + LLM.

Metric	Value
Krippendorff's α (nominal, 4 annotators)	0.497

Table 6: Pairwise agreement between humans and the LLM.

Annotator Pair	Percent Agreement	Cohen's κ
H1–LLM	62.8%	0.489
H2–LLM	62.5%	0.492
H3–LLM	59.7%	0.448

Overall, the dataset exhibits moderate inter-annotator consistency across all metrics, with variation typical of multi-class subjective labeling tasks. The LLM aligns with human labels at levels comparable to human–human agreement, and the LLM agrees more with H1 and H2, who have a higher inter-annotator agreement.

C TOKEN ROUTING PATTERNS

GPT-5 Prompt for Generating Expert Specific Stimuli Figure 10 presents the prompt used to instruct GPT-5 to generate the question–answer pairs shown in the non-benchmark token-routing pattern plots. The descriptions of the brain networks are identical to those in Figure 9, which were previously used to pseudo-label O1-generated responses for constructing the $\text{MICRO}_{\text{SFT}}$ dataset. We queried GPT-5 separately for each expert. We show the routing patterns for additional models in Figure 12 and for MOE models in Figure 17.

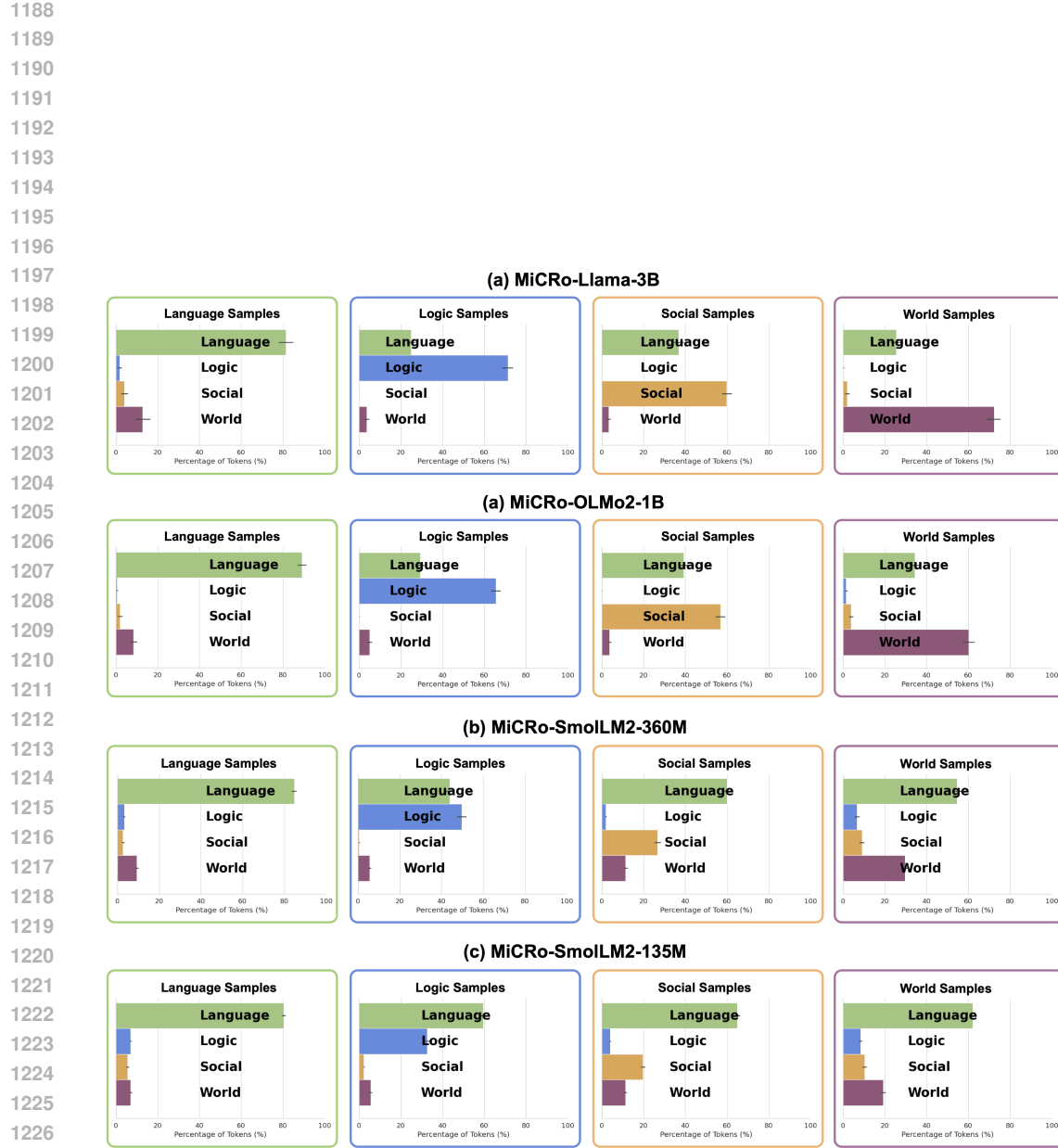


Figure 12: Token Routing Patterns in Additional MICRO-Models. Percentage of tokens routed to each expert, aggregated across all layers, for additional MICRO models. Distributions are computed over GPT-5-generated question–answer pairs designed to engage specific domains. Results show consistent brain-inspired specialization, with tokens preferentially assigned to the relevant experts depending on the task domain. Figure 13 shows the corresponding layer-wise token routing of these plots, while Figure 14 shows the token routing on benchmark testing data.

1242

1243

1244

1245

1246

1247

1248

1249

1250

1251

1252

1253

1254

1255

1256

1257

1258

1259

1260

1261

1262

1263

1264

1265

1266

1267

1268

1269

1270

1271

1272

1273

1274

1275

1276

1277

1278

1279

1280

1281

1282

1283

1284

1285

1286



Figure 13: **Layer-wise Token Routing in MiCRO Models.** Token routing distributions across layers for five MiCRO models, measured on GPT-5-generated question–answer pairs targeting specific domains. In all models, the language expert is consistently engaged in early layers, while domain-specific experts (logic, social, world) are increasingly activated in deeper layers. This hierarchical organization parallels findings from cognitive neuroscience, where linguistic processing precedes engagement of higher-level networks.

1292

1293

1294

1295

1296 **Layerwise Routing Patterns** Figure 13 illustrates layer-wise token routing patterns for five Mi-
 1297 CRO models. Surprisingly, consistent trend emerges: tokens are initially processed by the lan-
 1298 guage expert before being delegated to higher-level experts depending on the task domain. This
 1299 organization parallels findings in cognitive neuroscience, where the language network is engaged
 1300 early for virtually all linguistic input and then interfaces with other specialized networks (such as
 1301 multiple-demand or social cognition systems) depending on task demands (Fedorenko et al., 2024).
 1302 In Figure 14, we show benchmark-specific token routing patterns across layers as well. To probe so-
 1303 cial specialization directly, we also include evaluation on the EMPATHY benchmark (Buechel et al.,
 1304 2018), which primarily engages the social expert, further confirming the expected routing behavior
 1305 is generalizable across datasets.

1306 D CORRELATION WITH HUMAN JUDGMENTS

1307 We use a dataset of 1,000 six-word sentences from Tuckute et al. (2024), each annotated with human
 1308 ratings across several behavioral dimensions, collected independently of our routing framework. To
 1309 test correlations with human judgments, we selected features expected to align with specific experts:
 1310 GRAMMATICALITY and PLAUSIBILITY with the language expert, MENTAL STATES with the social
 1311 expert, and PHYSICAL OBJECTS and PLACES with the world expert. The dataset does not include
 1312 features relevant to the logic expert.

1313 To analyze these relationships, we divide each model into three layer segments (early, middle, late)
 1314 and averaged router probabilities within each segment. Figure 15 reports correlations between the
 1315 average routing probability of each expert and human ratings for MiCRO-LLAMA-3.2-1B and
 1316 MiCRO-LLAMA-3.2-3B. For both models and layer segments, mental state ratings correlate most
 1317 strongly with the social expert. Language expert probabilities correlate with GRAMMATICALITY
 1318 and PLAUSIBILITY, but primarily in early layers. PHYSICAL OBJECTS and PLACES correlate with
 1319 the world expert, while the logic expert shows no positive correlations (and in most cases negative
 1320 correlations) with these features. These findings suggest that our router exhibits a meaningful degree
 1321 of correspondence with human behavioral judgments.

1324 E ADDITIONAL EXPERT ABLATION RESULTS

1325 Figure 16 reports the effect of ablating individual experts, including the language expert, on bench-
 1326 mark performance for five MiCRO models. We find that the language expert is essential for most
 1327 tasks, while domain-specific experts—such as the logic expert for GSM8K and MINERVA MATH—
 1328 are also necessary to maintain performance. Interestingly, in some cases, ablating an expert im-
 1329 proves performance, suggesting that certain experts may interfere with more relevant ones, leading
 1330 to performance degradation when all are active.

1334 F BENCHMARKS

1337 **Table 7: Number of Shots and Samples Per Benchmark Used in Evaluation.** Number of shots
 1338 and samples used when evaluating the test-set of each benchmark. Last two row shows whether we
 1339 used CoT or evaluated using log-probabilities and the metric used to obtain the final accuracy.

Benchmark	GSM8K	Minerva Math	MMLU	MMLU-Pro	BBH	HellaSwag	PIQA	ARC _{Easy}	ARC _{Challenge}
N-Shots	0-Shot	4-shots	4-shots	5-shots	3-Shots	0-Shot	0-Shot	0-Shot	0-Shot
Num Samples	1,319	5,000	14,042	12,032 * 6,511	10,042	1,838	2,376	1,172	
CoT Prompting	Yes	Yes	Yes	Yes	Yes	No	No	No	No
Metric	Exact Match	Exact Match	Exact Match	Exact Match	Exact Match	Acc Norm	Acc Norm	Acc	Acc Norm

1344 **Benchmarks Description** We evaluate our models on eight benchmarks using various fewshot
 1345 settings, four of which are prompted to generate a reasoning chain before producing the final answer.
 1346 These reasoning steps are intended to more meaningfully engage the expert modules throughout the
 1347 generation process, which is why we focused on them in the main paper. The other benchmarks are
 1348 multiple choice questions where the most likely candidate—as measured by the log-probabilities
 1349 of the model—is taken as the prediction. Table 7 lists the number of in-context examples used

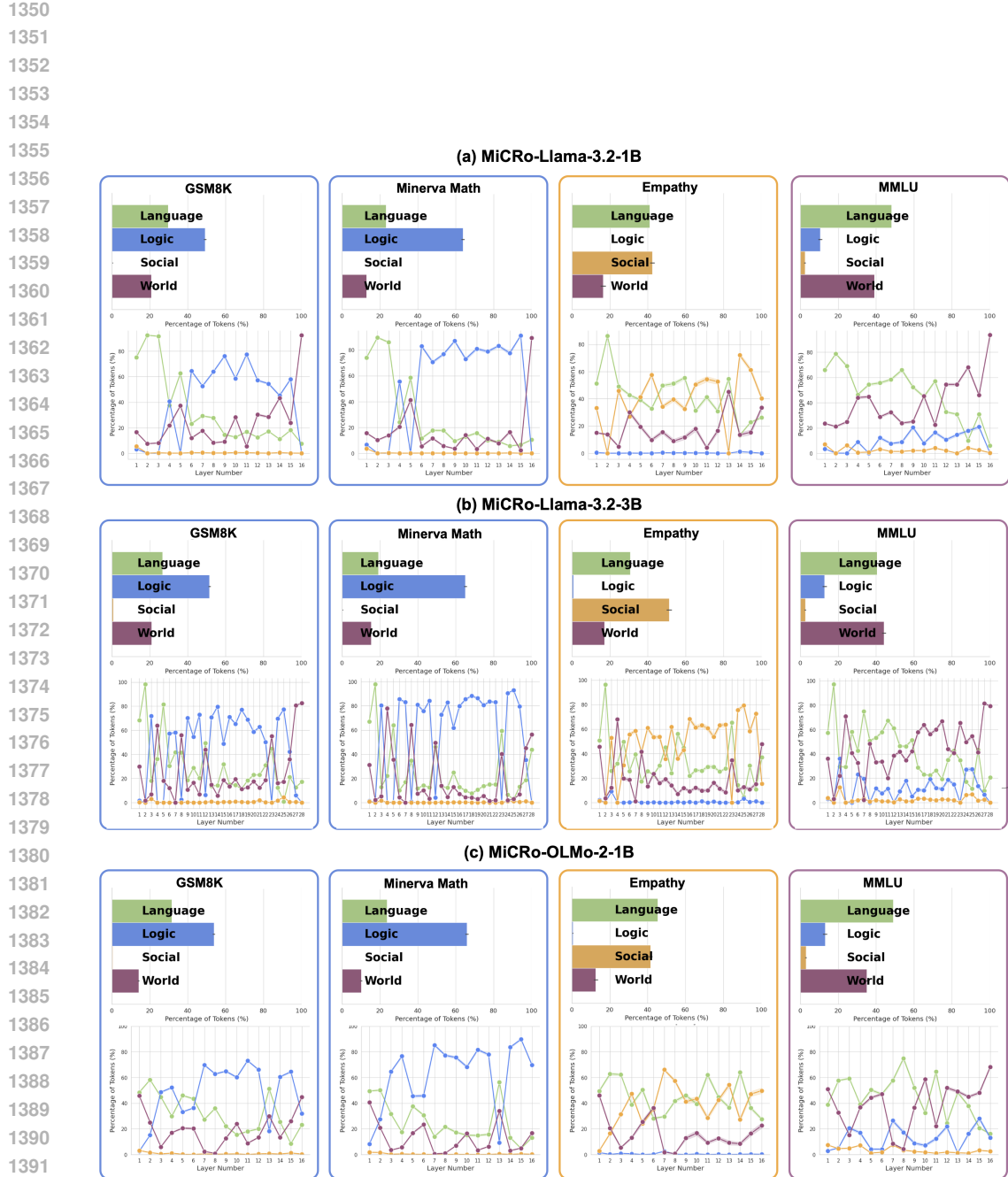


Figure 14: **Benchmark Token Routing Patterns.** Token routing patterns for (a) MiCRO-LLAMA-3.2-1B, (b) MiCRO-LLAMA-3.2-3B, and (c) MiCRO-OLMO-2-1B, evaluated on up to 1,000 samples drawn from the GSM8K, MINERVA-MATH, EMPATHY, and MMLU test sets. For each model, the top panel reports the overall percentage of tokens routed to each expert across the whole model (variance across samples), while the bottom panel shows layer-wise routing. The latter reveals an emergent hierarchy: earlier layers emphasize language grounding, whereas deeper layers increasingly delegate to domain-relevant experts.

1404

1405

1406

1407

1408

1409

1410

1411

1412

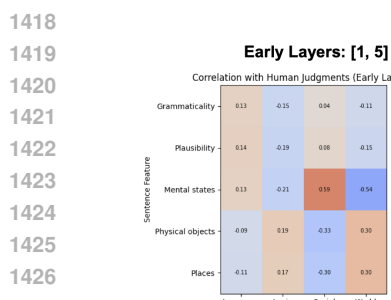
1413

1414

1415

1416

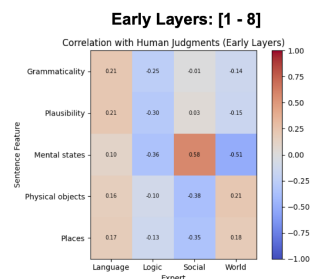
1417



(a) MiCRO-LLAMA-3.2-1B

Middle Layers: [6 - 10]

Late Layers: [11 - 16]



(b) MiCRO-LLAMA-3.2-3B

Middle Layers: [9 - 19]

Late Layers: [20 - 28]

Figure 15: **Correlations Between Expert Routing Probabilities and Human Ratings.** Correlations are shown for MiCRO-LLAMA-3.2-1B and MiCRO-LLAMA-3.2-3B, averaged across early, middle, and late layer segments. Mental state ratings correlate most strongly with the social expert, grammaticality and plausibility correlate to some degree with the language expert (primarily in early layers), and physical objects and places with the world expert. The logic expert shows no positive correlations with these features.

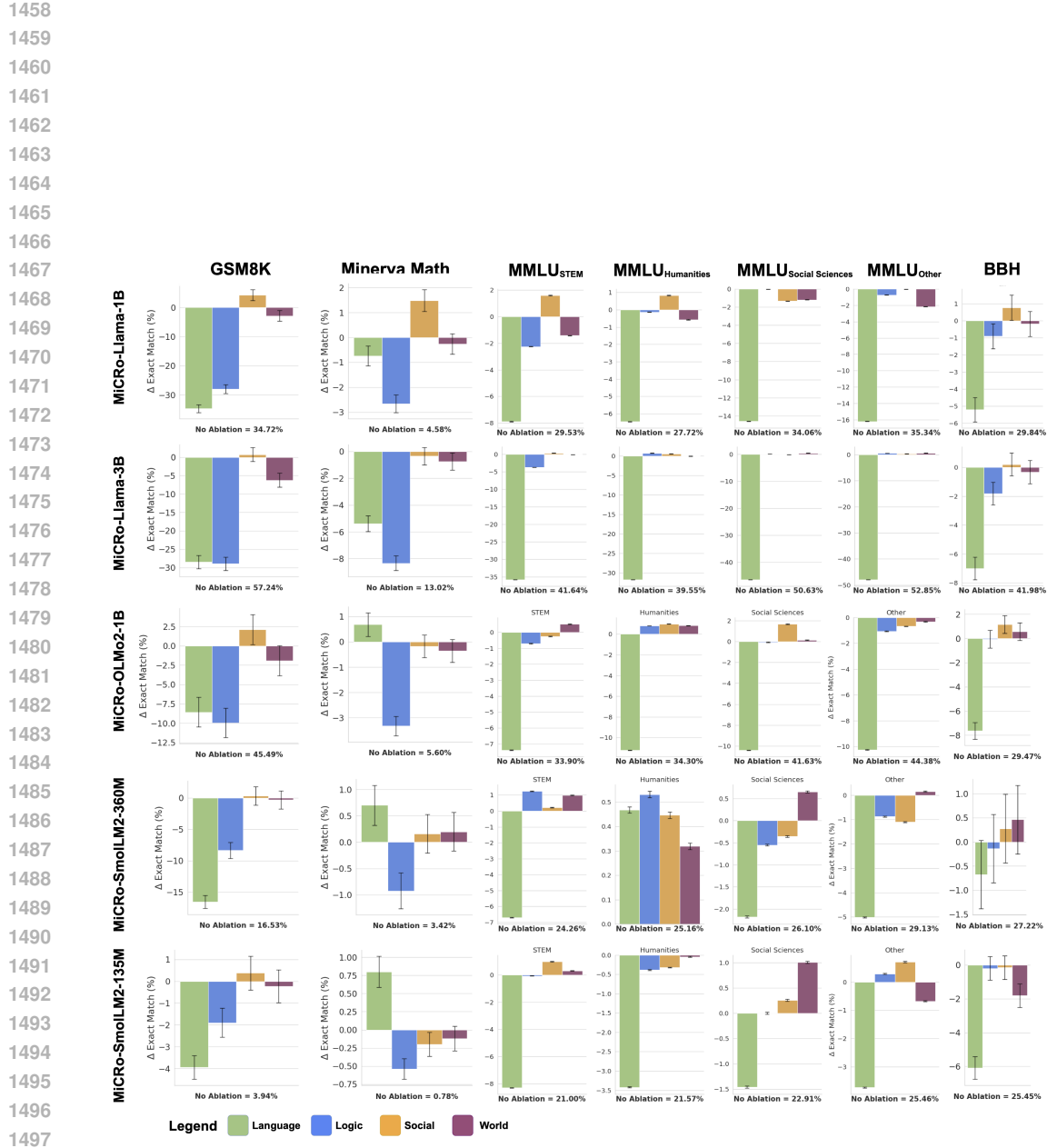


Figure 16: **Expert Ablation Results Across Benchmarks.** Impact of ablating individual experts on benchmark performance for five MiCRO models. Results are shown for GSM8K, MINERVA MATH, BBH, and MMLU, with the latter divided into its four subcategories. Removing the language expert causes substantial drops across most tasks, while domain-specific experts (e.g., logic for math benchmarks) are critical for their respective domains. In some cases, ablating an expert improves performance, suggesting interference with more relevant experts.

1512
 1513 **Table 8: Additional Benchmark Results for MiCRO and Baselines** Accuracy (%) \pm standard
 1514 error across reasoning and knowledge benchmarks. Results are reported for different model classes
 1515 (Dense, MoB, and MiCRO) under each base model.

Base Model	Model	GSM8K	Minerva	MMLU	MMLU _{Pro}	BBH	ARC _{Easy}	ARC _{Challenge}	HellaSwag	PIQA
SmollM2-135M	Dense	2.7 \pm 0.4	0.5 \pm 0.1	21.5 \pm 0.3	7.8 \pm 0.2	24.1 \pm 0.5	62.8 \pm 1.0	29.6 \pm 1.3	43.6 \pm 0.5	67.7 \pm 1.1
	MoB	3.0 \pm 0.5	0.6 \pm 0.1	21.9 \pm 0.3	7.4 \pm 0.2	23.5 \pm 0.5	63.0 \pm 1.0	29.9 \pm 1.3	43.5 \pm 0.5	67.8 \pm 1.1
	MiCRO	3.9 \pm 0.5	0.8 \pm 0.1	22.5 \pm 0.4	7.9 \pm 0.2	25.4 \pm 0.5	56.0 \pm 1.0	27.6 \pm 1.3	41.8 \pm 0.5	67.5 \pm 1.1
SmollM2-360M	Dense	15.0 \pm 1.0	3.7 \pm 0.3	26.4 \pm 0.4	9.9 \pm 0.3	27.3 \pm 0.5	69.7 \pm 0.9	37.5 \pm 1.4	56.6 \pm 0.5	71.4 \pm 1.1
	MoB	17.4 \pm 1.0	3.9 \pm 0.3	26.8 \pm 0.4	9.8 \pm 0.3	27.7 \pm 0.5	70.0 \pm 0.9	37.1 \pm 1.4	56.9 \pm 0.5	72.0 \pm 1.0
	MiCRO	16.5 \pm 1.0	3.4 \pm 0.3	26.0 \pm 0.4	10.1 \pm 0.3	27.2 \pm 0.5	69.9 \pm 0.9	38.2 \pm 1.4	56.7 \pm 0.5	71.7 \pm 1.1
Llama-3.2-1B	Dense	36.8 \pm 1.3	4.8 \pm 0.3	29.7 \pm 0.4	11.2 \pm 0.3	30.4 \pm 0.5	64.3 \pm 1.0	33.7 \pm 1.4	58.4 \pm 0.5	73.8 \pm 1.0
	MoB	30.5 \pm 1.3	3.7 \pm 0.3	27.1 \pm 0.4	11.0 \pm 0.3	27.4 \pm 0.5	61.7 \pm 1.0	32.4 \pm 1.4	56.2 \pm 0.5	71.3 \pm 1.1
	MiCRO	34.7 \pm 1.3	4.6 \pm 0.3	31.2 \pm 0.4	10.7 \pm 0.3	29.8 \pm 0.5	59.6 \pm 1.0	32.8 \pm 1.4	54.7 \pm 0.5	73.1 \pm 1.0
Llama-3.2-3B	Dense	58.0 \pm 1.4	14.4 \pm 0.5	48.6 \pm 0.4	19.6 \pm 0.4	44.1 \pm 0.6	73.6 \pm 0.9	42.9 \pm 1.4	68.9 \pm 0.5	77.0 \pm 1.0
	MoB	51.6 \pm 1.4	12.3 \pm 0.5	45.2 \pm 0.4	19.1 \pm 0.4	42.2 \pm 0.6	71.6 \pm 0.9	41.3 \pm 1.4	67.3 \pm 0.5	77.0 \pm 1.0
	MiCRO	57.2 \pm 1.4	13.0 \pm 0.5	45.4 \pm 0.4	19.0 \pm 0.4	42.0 \pm 0.6	73.0 \pm 0.9	43.3 \pm 1.4	67.4 \pm 0.5	76.6 \pm 1.0

1525
 1526 and the number of samples tested for each benchmark. For the remaining benchmarks, we used
 1527 the default fewshot examples from the lm-evaluation-harness (Gao et al., 2024) repository.
 1528 Specifically, we used the bbh_cot_fewshot task for BBH, the mmlu_flan_cot_fewshot task
 1529 for MMLU, the mmlu_pro for MMLU-PRO, the minerva_math task for MINERVA MATH, and
 1530 the gsm8k_cot_zeroshot for the GSM8K task. We used the default tasks for the multiple-
 1531 choice benchmarks.

1532
 1533 **Extended Benchmark Results** Table 8 reports results for additional base models as well as on
 1534 benchmarks beyond those presented in the main paper. Consistent with the main results, MiCRO
 1535 remains comparable to Dense and MoB baselines across most tasks while being interpretable. These
 1536 supplementary experiments provide further evidence that the observed trends hold across a broader
 1537 range of model scales and evaluation settings.

G ROBUSTNESS ACROSS POST-TRAINING METHODS

1541 We further assess the robustness of our method to different post-training methods by applying two
 1542 variations. First, we further post-train our MiCRO models using Direct Preference Optimization
 1543 (DPO) (Rafailov et al., 2023) on a subset of the TÜLU-2.5 preference dataset (Ivison et al., 2024)
 1544 (Table 9). Second, we replace the large-scale general-purpose TÜLU-3 dataset used in stage-3 with a
 1545 more domain-specific (medical) instruction-tuning set used in Bosselut et al. (2024) (Table 10). Our
 1546 results show that our method is robust to different post-training pipelines, whether applying DPO or
 1547 using an alternative instruction-tuning dataset, as shown in Tables 9 and 10 respectively.

1548
 1549 **Table 9: Performance After DPO Finetuning** Comparison of MiCRO models and baselines after
 1550 further finetuning with DPO on a preference dataset. Results show average performance across the
 1551 4 benchmarks, indicating that specialization remains beneficial after DPO.

Base Model	Model	GSM8K	Minerva Math	MMLU	BBH	Average
Llama-3.2-1B	Dense	38.1	3.9	29.4	30.3	25.4
	MiCRO	39.3	5.8	31.8	30.3	26.8
OLMo-2-1B	Dense	45.8	5.6	39.3	29.8	30.1
	MiCRO	48.1	5.8	39.8	30.4	31.0

H MIXTURE-OF-EXPERTS RESULTS

1562 In the main paper, we report results using the mixture-of-blocks (MoB) architecture, where each
 1563 expert is a full transformer block with its own attention mechanism. Here, we contrast these results
 1564 with the more standard mixture-of-experts (MoE) architecture, where experts consist only of FFN
 1565 blocks and attention is shared across experts within each layer. We first present routing patterns for
 MiCRO-MoE models, highlighting cases where our training curriculum fails to induce the intended

1566

Table 10: **Performance on Medical Benchmarks After Domain-Specific Instruction Tuning.** Models are finetuned during Stage-3 using a medical instruction-tuning dataset instead of TÜLU-3, and evaluated on four medical benchmarks. Results show that specialization achieve competitive performance across both base models, and outperforming in the out-of-distribution (OOD) setting. We choose the option with the highest log-probability among the multiple-choice options.

Base Model	Model	Out-of-Distribution		In-Distribution		Average	
		MMLU	Medicine	MedQA	MedMCQA		
Llama-3.2-1B	Dense	26.0		34.3	33.9	73.4	41.9
	MiCRO	28.3		35.2	33.9	71.4	42.2
OLMo-2-1B	Dense	35.8		34.2	35.3	74.0	44.8
	MiCRO	35.8		36.3	34.5	73.8	45.1

1579

1580

Table 11: **Results with Mixture-of-Experts (MoE) Architectures.** Accuracy (%) \pm standard error is reported for Dense, MoE, and MiCRO-MoE models across multiple benchmarks. For each base model, the best score per benchmark is highlighted in bold.

Base Model	Model	GSM8K	Minerva	MMLU	BBH	ARC _{Easy}	ARC _{Challenge}	HellaSwag	PIQA
SmollM2-135M	Dense	2.7 \pm 0.4	0.5 \pm 0.1	21.5 \pm 0.3	24.1 \pm 0.5	62.8 \pm 1.0	29.6 \pm 1.3	43.6 \pm 0.5	67.7 \pm 1.1
	MoE	2.8 \pm 0.5	0.6 \pm 0.1	22.3 \pm 0.3	24.6 \pm 0.5	62.9 \pm 1.0	29.4 \pm 1.3	43.6 \pm 0.5	67.6 \pm 1.1
	MiCRO-MoE	4.1 \pm 0.5	0.4 \pm 0.1	22.2 \pm 0.3	24.5 \pm 0.5	62.0 \pm 1.0	29.0 \pm 1.3	43.4 \pm 0.5	67.5 \pm 1.1
SmollM2-360M	Dense	15.0 \pm 1.0	3.7 \pm 0.3	26.4 \pm 0.4	27.3 \pm 0.5	69.7 \pm 0.9	37.5 \pm 1.4	56.6 \pm 0.5	71.4 \pm 1.1
	MoE	16.1 \pm 1.0	3.6 \pm 0.3	26.6 \pm 0.4	27.4 \pm 0.5	70.2 \pm 0.9	37.2 \pm 1.4	56.8 \pm 0.5	71.8 \pm 1.1
	MiCRO-MoE	16.1 \pm 1.0	4.0 \pm 0.3	26.1 \pm 0.4	27.0 \pm 0.5	69.7 \pm 0.9	37.5 \pm 1.4	56.7 \pm 0.5	71.4 \pm 1.1
Llama-3.2-1B	Dense	36.8 \pm 1.3	4.8 \pm 0.3	29.7 \pm 0.4	30.4 \pm 0.5	64.3 \pm 1.0	33.7 \pm 1.4	58.4 \pm 0.5	73.8 \pm 1.0
	MoE	29.1 \pm 1.3	4.7 \pm 0.3	25.7 \pm 0.4	28.6 \pm 0.5	64.1 \pm 1.0	35.2 \pm 1.4	57.9 \pm 0.5	72.5 \pm 1.0
	MiCRO-MoE	35.4 \pm 1.3	5.0 \pm 0.3	30.4 \pm 0.4	30.1 \pm 0.5	65.0 \pm 1.0	35.5 \pm 1.4	57.3 \pm 0.5	73.8 \pm 1.0

1592

1593

1594

specialization—an issue we primarily observe in models larger than 1.5B parameters. We then report the performance of the models that did exhibit specialization on reasoning benchmarks.

1597

1598

H.1 MOE TOKEN ROUTING PATTERNS

1599

Figure 17 shows routing patterns for five MiCRO-MoE models on question–answer pairs generated with GPT-5 to target specific experts. The MiCRO-MoE-LLAMA-1B model exhibits the intended specialization, whereas the 3B variant does not. Within the SMOLLM2 family, the 135M and 360M models display partial specialization, though less cleanly than LLAMA-1B, often defaulting to the language expert regardless of the input domain. The 1.7B model fails to specialize, similar to MiCRO-MoE-LLAMA-3B, indicating that the MoE architecture does not reliably induce the desired specialization under our training curriculum.

1607

1608

1609

H.2 MOE BENCHMARK RESULTS

1610

1611

Table 11 presents results for models trained with a Mixture-of-Experts (MoE) design, complementary to the Mixture-of-Blocks (MoB) results reported in the main paper. The key distinction between MoE and MoB lies in what is replicated to form the experts. In standard MoE, only the feed-forward network (FFN) within each layer is cloned into multiple experts, with the self-attention module shared across all experts. In contrast, MoB duplicates the entire transformer block—including both the attention and FFN components—so that each expert has its own attention mechanism as well as its own FFN. We find that MoB scales more effectively: under our training curriculum, specialization emerges reliably in larger models ($> 1\text{B}$ parameters) for MoB, but not for MoE. For this reason, we focus on MoB in the main text and do not include the MoE variants of the other base models, as they did not exhibit the expected functional specialization.

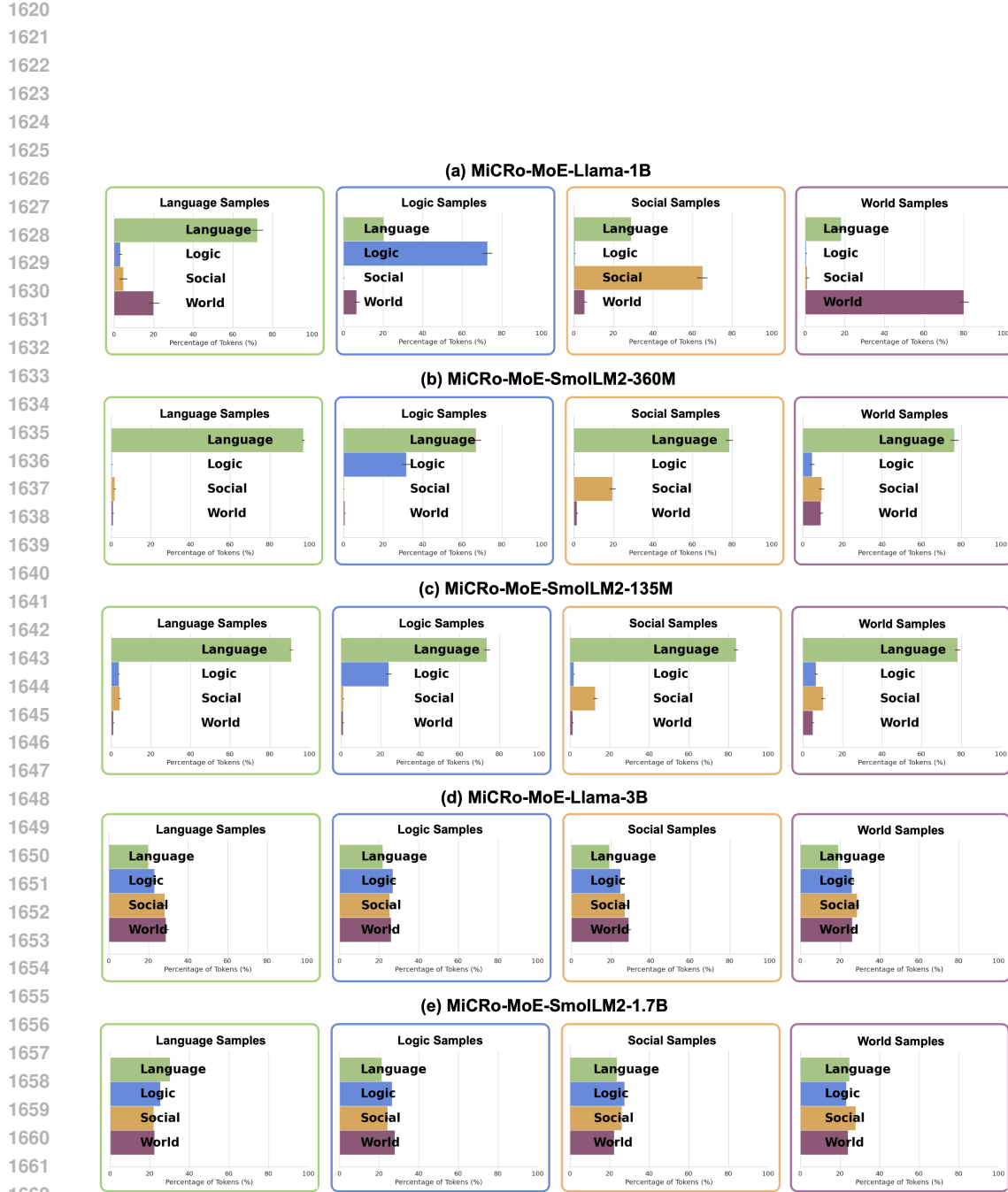


Figure 17: **Routing Patterns in MiCRO-MoE Models.** Routing behavior for five MiCRO-MoE models on GPT-5-generated question–answer pairs targeting specific experts. The MiCRO-MoE-LLAMA-1B model shows the intended specialization, while larger variants (e.g., 3B, SmoILM2-1.7B) fail to specialize. Smaller SMoILM2 models (135M and 360M) display partial but less consistent specialization, often defaulting to the language expert. These results suggest that the MoE architecture does not reliably induce brain-like specialization under our training curriculum.

1674

1675 Table 12: Performance of MiCRO-OLMo-1B when increasing the number of active experts from
 1676 Top-1 to Top-2 at test time. Enabling an additional expert leads to consistent improvements across
 1677 most benchmarks, demonstrating that the model generalizes well to increased routing capacity even
 1678 though SFT was performed with Top-1 routing. The benchmarks MATH, ARC-E, and ARC-C
 1679 refer to MINERVA-MATH, ARC-EASY, and ARC-CHALLENGE respectively.

K	GSM8K	BBH	MMLU	MATH	HellaSwag	PIQA	ARC-E	ARC-C	Avg
1	45.5%	29.5%	37.9%	5.6%	65.4%	75.2%	70.2%	41.3%	46.3%
2	47.7%	30.6%	38.2%	6.8%	66.4%	75.4%	71.9%	41.6%	47.3%

1683

1684

I ADDITIONAL BEHAVIORAL ALIGNMENT RESULTS

1685 Figure 18 shows alignment to human behavior for additional base models, comparing MiCRO with
 1686 corresponding MOB and DENSE baselines. We find that MiCRO achieves higher average behavioral
 1687 alignment on COGBENCH metrics in larger models, while maintaining comparable performance in
 1688 smaller models. Please refer to §5.4 for more details on how we evaluate the models.

1689

J SPECIALIZATION REMAINS CONSISTENT THROUGHOUT TRAINING

1690 Figure 19 illustrates token routing assignments across checkpoints during Stage 3 training of
 1691 MiCRO-LLAMA-1B, with checkpoint-0 representing the final weights from Stage 2. The results
 1692 show that the model consistently preserves the specialization established in stages 1 and 2, despite
 1693 no explicit constraints being enforced during this phase, except for the initial weak inductive bias.
 1694 This suggests that brain-like specialization may offer a robust initialization, enabling the model to
 1695 maintain functionally distinct expert behaviors throughout continued end-to-end training.

1696

1697

1698

1699

1700

1701

1702

K QUALITATIVE EXAMPLES OF STEERING BEHAVIOR

1703 Figures 22-25 show examples of how one can use MiCRO to steer the model’s behavior by selec-
 1704 tively ablating or activating certain experts. In the examples provided, we only retain the target
 1705 expert along with the language expert using the MiCRO models. When the social expert is ablated,
 1706 the model shifts toward a more analytical tone, producing a response that is logically coherent but
 1707 lacking in empathy.

1708

1709

1710

L TEST-TIME SCALING BY INCREASING THE NUMBER OF ACTIVE EXPERTS

1711 Table 12 reports the effect of increasing the number of active experts at test time from 1 to 2 for
 1712 MiCRO-OLMo-1B. The results show that test-time compute can be scaled by enabling additional
 1713 experts, and that the model generalizes well to this setting and improves performance on all bench-
 1714 marks, even though the large-scale SFT stage was trained exclusively with top-1 routing. This
 1715 indicates that MiCRO retains robustness when the routing capacity is expanded at inference time
 1716 under the $k=2$ setting. However, with larger values of k the performance degrades slightly.

1717

1718

M SCALING MiCRO TO LLAMA-3.1-8B BASE MODEL

1719

1720

1721

1722

1723

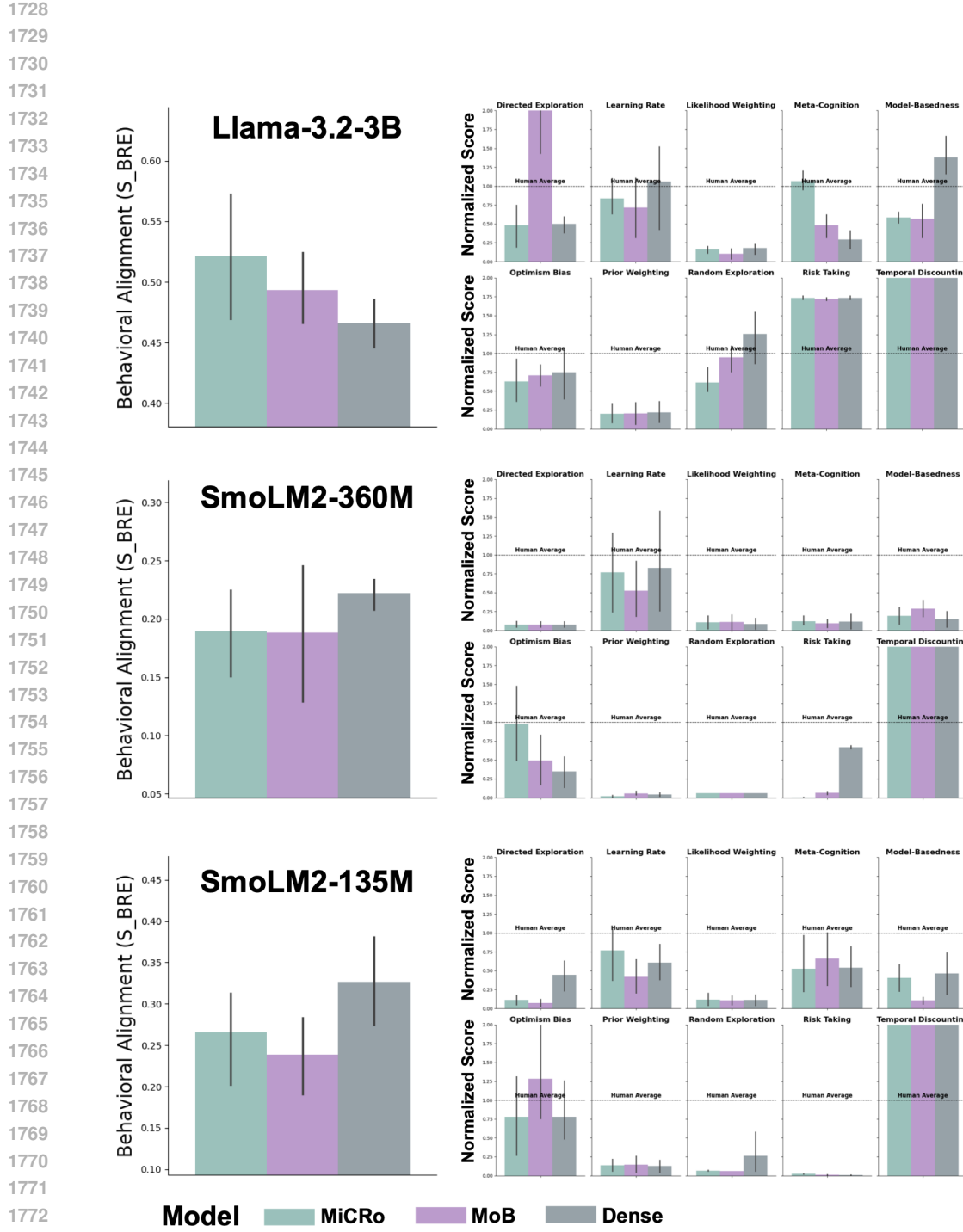
1724

1725

1726

1727

We post-trained three Llama-3.1-8B variants: (1) MiCRO-LLAMA-8B, (2) its modular baseline
 LLAMA-8B-MOB, and (3) LLAMA-8B-DENSE. However, due to compute constraints, we instantiated
 experts only in the last 12 layers of MiCRO-LLAMA-8B and LLAMA-8B-MOB, keeping the
 earlier layers dense. This choice is motivated by our prior findings (Figures 13–14), which show that
 early layers predominantly route to language experts, while non-language specializations emerge in
 later layers. The results confirm that MiCRO-LLAMA-8B exhibits the expected routing patterns in
 its last 12 layers, as shown in Figure 20. Table 13 shows the results on 9 benchmarks of the three
 LLAMA-3.1-8B model variants, along with the results when we remove the most detrimental ex-
 pert across all layers for a given task for the MiCRO and MOB models. Using a paired Wilcoxon



1775 **Figure 18: Behavioral Alignment on Additional Base Models.** Results for LLAMA-3.2-3B,
1776 SMOLLM2-360M, and SMOLLM2-135M on COGBENCH. Left: average similarity to human
1777 behavior across all metrics. Right: fine-grained results for each behavioral metric. MiCRO is
1778 compared with MOB and DENSE baselines, showing stronger alignment in larger models and com-
1779 parable performance in smaller ones.

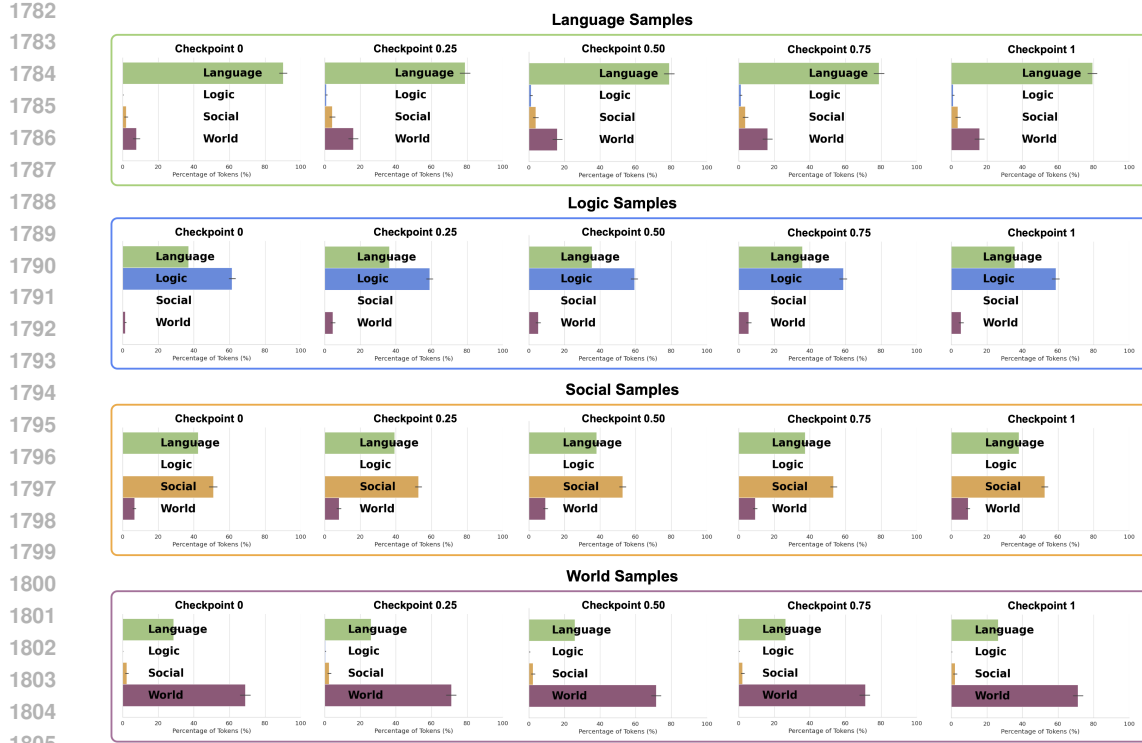


Figure 19: **Specialization Remains Consistent Throughout Training.** Token routing across checkpoints during Stage 3 training of MiCRO-LLAMA-1B on the samples generated to probe each corresponding expert. Checkpoint 0 corresponds to the final weights from Stage 2. The plot shows that expert assignments remain stable throughout training, with minimal variation, indicating that the model retains its learned specialization despite the absence of explicit constraints.

Table 13: **Benchmark Results for Llama-3.1-8B Model Variants.** Performance comparison of LLAMA-3.1-8B variants across multiple benchmarks. Ablation refers to selectively removing the least relevant expert per benchmark.

Model Name	GSM8K	BBH	MMLU	MMLU Pro	MATH	HellaSwag	PIQA	ARC-E	ARC-C	Avg
Llama-8B-Dense	71.3	54.2	51.6	24.6	21.5	72.8	78.3	74.3	44.1	54.7
Llama-8B-MoB	69.3	54.1	52.0	23.5	21.3	72.2	78.9	74.6	46.9	54.8
Llama-8B-MoB (Ablation)	70.0	55.9	54.1	36.3	21.6	72.4	79.3	75.0	46.9	56.8
MiCRO-LLAMA-8B	69.1	53.6	50.7	23.1	18.1	72.7	78.7	75.7	45.9	54.2
MiCRO-LLAMA-8B (Ablation)	69.1	55.0	52.7	36.3	18.2	73.1	78.7	76.3	46.7	56.2

signed-rank test across the nine benchmarks, we find no statistically significant difference between MiCRO and either of the two baselines. The DENSE vs. MiCRO comparison yields a test statistic of 31.0 ($p = 0.18$), and the MoB vs. MiCRO comparison yields 33.5 ($p = 0.10$), both well above the conventional 0.05 significance threshold. However, when we ablate the most detrimental expert per task for both MiCRO and MoB we see a jump in performance, as also illustrated in Figure 7. In general, the Llama-8B experiments confirm our initial results that MiCRO remains competitive on a suite of benchmarks while remaining interpretable and relevant to cognitive neuroscience.

N LARGE LANGUAGE MODEL USAGE

We used large language models (LLMs) solely for editing and grammatical refinement of the manuscript. All substantive ideas, analyses, and conclusions presented in this work are our own.

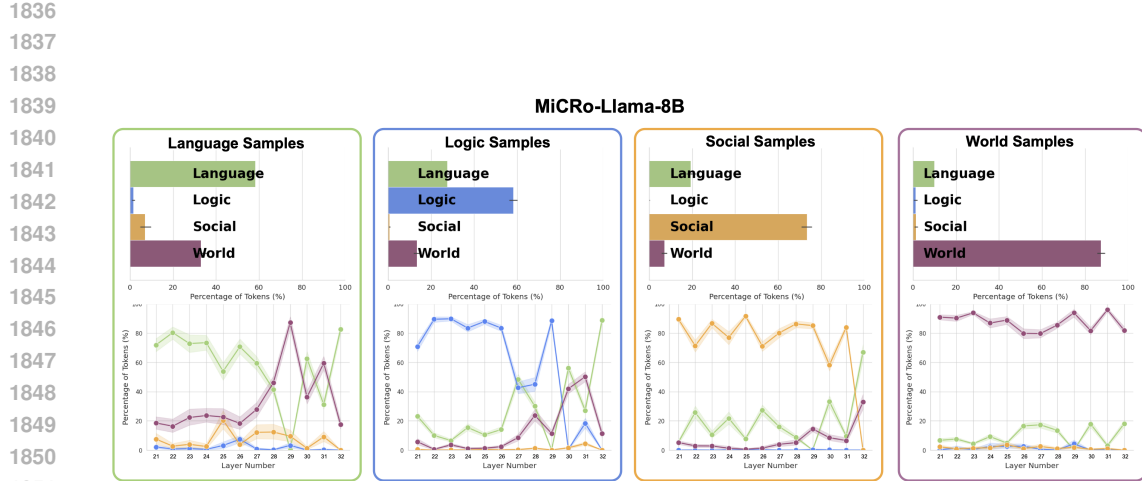


Figure 20: **Token Routing Patterns for MiCRO-Llama-8B.** (Top) The percentage of tokens routed to each expert aggregated across the last 12 layers of MiCRO-Llama-8B. The samples are GPT-5 generated question-answer pairs targeting specific domains. (Bottom) The corresponding layer-wise token routing patterns.

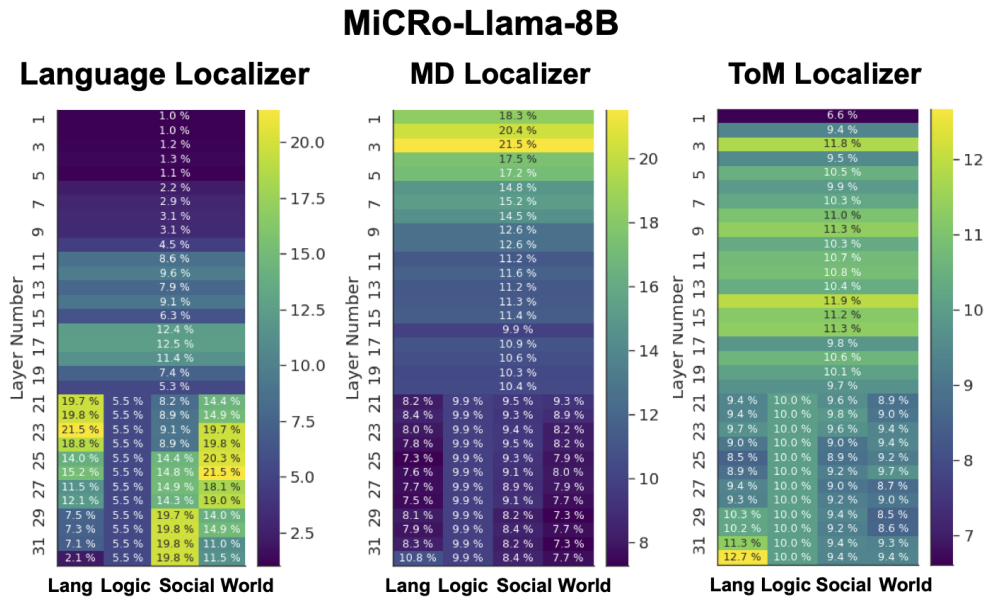


Figure 21: **Neuroscience Localizers Fail to Recover Experts For Hybrid MiCRO-Llama-8B**
 Following the procedure in Figure 5, we apply three neuroscience-inspired functional localizers to MiCRO-Llama-8B, which places experts only in the final 12 layers due to compute constraints. In contrast to the full MiCRO variants with experts in every layer, the localizers are unable to reliably recover the expected expert specializations in this hybrid configuration.

1890
 1891
 1892
 1893
 1894
 1895
Prompt
 1896 If two people disagree on how to split \$10 fairly, what should they do?
 1897
 1898
All Experts
 1899 If two people disagree on how to split \$10 fairly, they should try to find a compromise that satisfies both parties. This could
 1900 involve discussing the different ways of splitting the money and finding a solution that is fair to both of them. It's important to
 1901 remember that the goal is to reach a fair and equal agreement, so both parties should be willing to work together to find a
 1902 solution.
 1903
Logic
 1904 If two people disagree on how to split \$10 fairly, they should try to find a compromise that both can agree on. They can do
 1905 this by trying to find a number that both people can agree on, such as the average of the two numbers, or by trying to find
 1906 a number that is closer to both numbers than either number itself.
 1907
Social
 1908 If two people disagree on how to split \$10 fairly, they should try to find a compromise that satisfies both parties. Here are
 1909 some steps they can take:
 1910
 1. **Communicate openly**: Both parties should express their opinions and listen to each other's perspectives. This will
 1911 help them understand each other's viewpoints and find common ground.
 1912
 2. **Find common ground**: Look for areas of agreement or values that both parties share. This will help them find a
 1913 compromise that is fair to both of them.
 1914
 3. **Discuss the reasons behind their disagreement**: Ask both parties why they disagree on how to split \$10 fairly. This
 1915 will help them understand each other's perspectives and find a solution that satisfies both parties.
 1916
 4. **Explore alternative solutions**: If they cannot find a compromise that satisfies both parties, they can explore alternative
 1917 solutions, such as splitting the money in a different way or finding a different way to split the money fairly.
 1918
 5. **Seek help from a mediator**: If the disagreement is too difficult to resolve on their own, they can seek help from a
 1919 mediator, such as a family member, friend, or counselor, to help them find a solution that is fair to both parties.
 1920
 6. **Find a solution that works for both parties**: Ultimately, they should find a solution that works for both parties and is fair
 1921 to both of them. This may involve compromising on certain points or finding a different way to split the money fairly.
 1922
World
 1923 If two people disagree on how to split \$10 fairly, they should consider the following options:
 1924
 1. **Mediation**: One person can mediate the disagreement by suggesting a compromise or a fair split. This can help both
 1925 parties reach an agreement without further conflict.
 1926
 2. **Negotiation**: Both parties can negotiate a fair split by discussing the benefits and drawbacks of different splits. They can
 1927 try to find a solution that both parties can agree on.
 1928
 3. **Arbitration**: If the disagreement is significant and cannot be resolved through mediation or negotiation, both parties can
 1929 seek the help of a neutral third party, such as a mediator or arbitrator, to help them reach an agreement.
 1930
 4. **Legal action**: If the disagreement is not resolved through mediation or negotiation, both parties can consider seeking
 1931 legal advice or taking legal action to enforce their rights.
 1932
 5. **Consultation**: Both parties can consult with a neutral third party, such as a financial advisor or mediator, to help them
 1933 reach a fair split. This can provide a neutral perspective and help both parties reach an agreement.
 1934
 Ultimately, the best course of action depends on the specific circumstances of the disagreement and the preferences of the
 1935 parties involved.
 1936
 1937
Figure 22: Example for Steering Model Behavior by Expert Ablation. Responses of M1CRO-
 1938 LLAMA-3B to the given prompt when only the target expert and the language expert are retained.
 1939 The differences illustrate the causal role of each expert and demonstrate how ablations can steer the
 1940 model's behavior.
 1941
 1942
 1943

1944

1945

1946

1947

1948

1949

1950

1951

1952

1953

1954

1955

Prompt

If your friend asks whether you like their new haircut, but you don't, what should you say?

1956

1957

All Experts

You can say something like, "I appreciate your creativity, but I don't think this is the style for me."

1958

1959

1960

1961

1962

Logic

You can say something like, "I'm glad you're happy with it, but I'm not a fan of it myself."

1963

1964

1965

1966

Social

When your friend asks if you like their new haircut, but you don't, it's important to be honest and respectful. Here's a suggestion on how to respond:

1967

1968

1969

1. **Be Honest**: You can say something like, "I really appreciate your style, but this particular haircut isn't for me. I think it's a great choice for you, though."

1970

1971

2. **Compliment**: If you do like something about their new look, make sure to compliment it. For example, "I love your hair color. This new cut just isn't for me."

1972

1973

3. **Express Your Feelings**: If you're not a fan of the haircut, you can say something like, "I just don't think this particular style works for me. I'm sure it's going to be a hit with you."

1974

1975

4. **Offer Support**: If your friend is disappointed, offer your support. "I know you're disappointed, but I'm sure you'll find something you love."

1976

1977

Remember, it's important to be kind and understanding, even if you don't like the haircut. It's also okay to be honest about your feelings.

1978

1979

1980

1981

World

You can say something like, "I'm sorry, but I don't really like it."

1982

1983

1984

1985

1986

1987

1988

1989

Figure 23: **Example for Steering Model Behavior by Expert Ablation.** Responses of MICRO-LLAMA-3B to the given prompt when only the target expert and the language expert are retained. The differences illustrate the causal role of each expert and demonstrate how ablations can steer the model's behavior.

1990

1991

1992

1993

1994

1995

1996

1997

1998
 1999
 2000
 2001
 2002
 2003
 2004
 2005
 2006
 2007
 2008
 2009
 2010
 2011
 2012
 2013
 Your friend is late to a meeting. Why might that be?
 2014
 2015
 2016
 2017
 2018
 Your friend might be late to a meeting for a variety of reasons. They could be running late, they might have forgotten their keys, or they could be in a rush to get to the meeting. It's important to remember that it's not always possible to avoid being late, and it's important to respect your friend's time and space.
 2019
 2020
 2021
 2022
 Your friend might be late to a meeting because they are late to work, or they are late to the bus, or they are late to the train, or they are late to the airport...
 2023
 2024
 2025
 2026
 2027
 2028
 Your friend might be late to a meeting for various reasons. They could be late due to a personal emergency, they might be late because they are not ready to meet, or they could be late due to a lack of preparation. It's important to approach this situation with empathy and understanding.
 2029
 2030
 2031
 2032
 2033
 2034
 Your friend might be late to a meeting for a variety of reasons. They could be running late, they might be waiting for someone else, or they could be experiencing a delay in their usual schedule. It's important to remember that being late can be frustrating and may not be a good reflection of your friend's character or reliability.
 2035
 2036
 Figure 24: **Example for Steering Model Behavior by Expert Ablation.** Responses of MiCRO-LLAMA-1B to the given prompt when only the target expert and the language expert are retained. The differences illustrate the causal role of each expert and demonstrate how ablations can steer the model's behavior.
 2037
 2038
 2039
 2040
 2041
 2042
 2043
 2044
 2045
 2046
 2047
 2048
 2049
 2050
 2051

2052

2053

2054

2055

2056

2057

2058

2059

2060

2061

2062

2063

2064

2065

2066

2067

2068

2069

2070

2071

2072

2073

2074

2075

2076

2077

2078

2079

2080

2081

2082

2083

2084

2085

2086

2087

2088

2089

2090

2091

2092

2093

2094

2095

2096

2097

2098

2099

2100

2101

2102

2103

2104

2105

Prompt

How could two people decide who gets the last slice of pizza?

All Experts

Two people could decide who gets the last slice of pizza by using a fair and unbiased method. Here are a few suggestions:

1. Random draw: One person could draw a random number between 1 and 2, and the other person would get the last slice if their number is 1.
2. Coin flip: One person could flip a coin, and the other person would get the last slice if the coin lands on heads.
3. Rolling dice: One person could roll a pair of dice, and the other person would get the last slice if the sum of the dice is even.
4. Drawing cards: One person could draw a card from a deck, and the other person would get the last slice if the card is a number between 1 and 2.
5. Using a fair method: One person could use a fair method, such as a coin flip or a random draw, to determine who gets the last slice of pizza.

It is important to ensure that the method used to determine who gets the last slice of pizza is fair and unbiased, so that both people feel that the decision is made in good faith.

Logic

To decide who gets the last slice of pizza, you can use a variety of methods. One way is to take turns picking the last slice. Another way is to flip a coin or use a random method to determine who gets the last slice. Remember, it's important to respect each other's choices and enjoy the pizza together.

Social

When deciding who gets the last slice of pizza, it's important to consider the following factors:

1. **Relationship and history**: If you have a history of sharing pizza or have a close relationship with the other person, they may be more likely to share the last slice with you.
2. **Current mood and energy**: If you're feeling particularly energetic or in a good mood, you may be more likely to share the last slice of pizza with the other person.
3. **Physical appearance**: If you're physically more capable or have a better sense of balance, you may be more likely to share the last slice of pizza with the other person.
4. **Emotional state**: If you're feeling particularly happy or content, you may be more likely to share the last slice of pizza with the other person.
5. **Situational context**: If you're in a particular situation or context, such as being in a group or having a specific reason for sharing pizza, you may be more likely to share the last slice of pizza with the other person.
6. **Nonverbal cues**: If you're using nonverbal cues, such as a smile or a friendly gesture, you may be more likely to share the last slice of pizza with the other person.
7. **Communication**: If you're communicating with the other person, you may be able to convey your intentions or desires more effectively, which could lead to a more positive outcome.
8. **Physical proximity**: If you're physically closer to the other person, you may be more likely to share the last slice of pizza with them.
9. **Personal values**: If you have a strong sense of fairness or equality, you may be more likely to share the last slice of pizza with the other person.
10. **Social norms**: If you're in a particular social group or community, there may be established norms or expectations regarding sharing

World

Your friend might be late to a meeting for a variety of reasons. They could be running late, they might be waiting for someone else, or they could be experiencing a delay in their usual schedule. It's important to remember that being late can be frustrating and may not be a good reflection of your friend's character or reliability.

Figure 25: **Example for Steering Model Behavior by Expert Ablation.** Responses of MiCRO-LLAMA-3B to the given prompt when only the target expert and the language expert are retained. The differences illustrate the causal role of each expert and demonstrate how ablations can steer the model's behavior.